One Earth

Article

Eco-friendly active film and sealant for underwater drug delivery to diseased corals

Graphical abstract

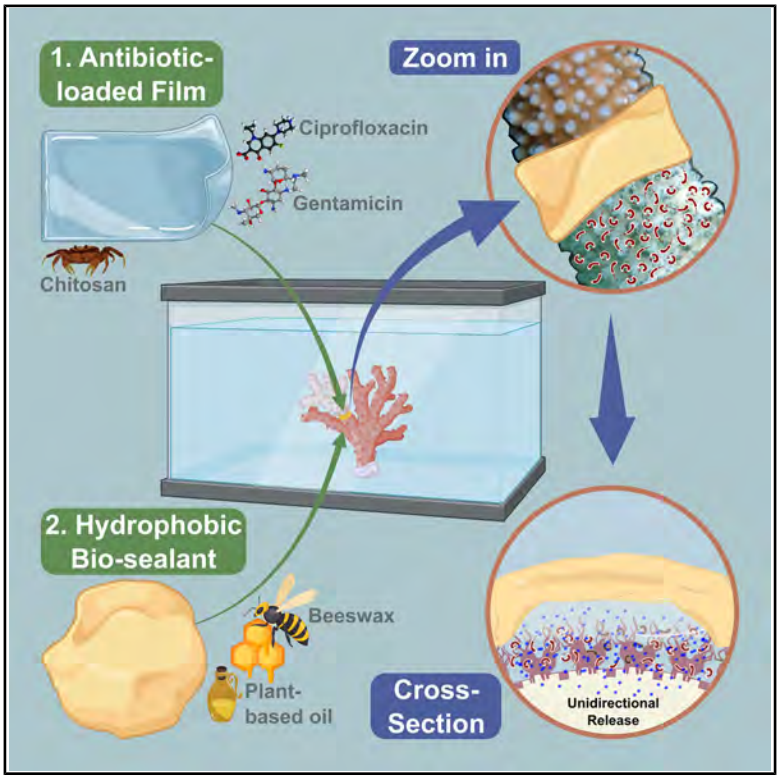

Highlights

- Hydrophilic films loaded with drugs and a bio-based hydrophobic sealant are used
- The system is designed to avoid drug leaks into the environment
- The films were effective against *Vibrio coralliilyticus*
- This treatment was successful in treating a coral tissue-necrosis-like disease

Authors

Vincenzo Scribano, Marco Contardi, Camilla Rinaldi, ..., Paolo Galli, Simone Montano, Athanassia Athanassiou

Correspondence

marco.contardi@unimib.it (M.C.), simone.montano@unimib.it (S.M.), athanassia.athanassiou@iit.it (A.A.)

In brief

Coral diseases are a major threat to coral reef ecosystems worldwide. Currently, only a few therapies have been found. To address this lack, this work presents an eco-friendly two-step system based on an antibiotic-loaded hydrophilic film and a thermoresponsive sealant that effectively inhibits coral pathogen growth, such as *Vibrio coralliilyticus*, and blocks the progression of tissue-necrosis-like disease.

Scribano et al., 2025, One Earth *8*, 101356
July 18, 2025
https://doi.org/10.1016/j.oneear.2025.101356

CellPress

One Earth

CellPress
OPEN ACCESS

Article

Eco-friendly active film and sealant for underwater drug delivery to diseased corals

Vincenzo Scribano,[1,2] Marco Contardi,[2,3,7,*] Camilla Rinaldi,[1,2] Valerio Isa,[2,3] Fabrizio Fiorentini,[1] Luca Ceseracciu,[4] Isabella Gandolfi,[2] Isabella Ghizzi,[2] Silvia Lavorano,[5] Paolo Galli,[2,3] Simone Montano,[2,3,6,*] and Athanassia Athanassiou[1,6,*]

[1]Smart Materials, Istituto Italiano di Tecnologia, 16163 Genova, Italy
[2]Department of Earth and Environmental Sciences (DISAT), University of Milano – Bicocca, 20126 Milan, Italy
[3]MaRHE Center (Marine Research and High Education Center), Magoodhoo Island, Faafu Atoll 12030, Republic of Maldives
[4]Materials Characterization Facility, Istituto Italiano di Tecnologia, 16163 Genova, Italy
[5]Costa Edutainment SpA – Acquario di Genova, 16128 Genova, Italy
[6]These authors contributed equally
[7]Lead contact
*Correspondence: marco.contardi@unimib.it (M.C.), simone.montano@unimib.it (S.M.), athanassia.athanassiou@iit.it (A.A.)
https://doi.org/10.1016/j.oneear.2025.101356

SCIENCE FOR SOCIETY Coral reefs are of great economic and ecological importance, contributing significantly to local economies through tourism and fishing. However, the impact of climate change, particularly the rise in seawater temperatures, has put these vital ecosystems at risk. The increased stress on coral reefs can lead to weakened immunity, making them susceptible to disease outbreaks. To address this issue a novel technology has been developed, drawing on knowledge from biomedicine, materials science, and ecology. This innovative tool aims to treat coral infections *in situ* and, at the same time, minimize potential ecological damage caused by the dispersion of antibiotics into the environment. It could also be readily utilized to control disease diffusion in intensive coral farms, such as *ex-situ* nurseries and aquaria. Furthermore, this technology holds potential for the preservation of ancient corals, which are of significant interest in scientific, ecological, and recreational spheres.

SUMMARY

Coral disease outbreaks have become a persistent threat to reefs, being more frequent and destructive in affecting these natural ecosystems but also coral nurseries and the aquaria business. To prevent catastrophic scenarios, effective technologies to treat outbreaks must be promptly implemented. We developed an eco-friendly underwater drug-delivery system to efficiently treat bacterial infections in corals. This system, composed of a hydrophilic film with 1% (w/w) antibiotic and a hydrophobic bio-based sealant, can be easily applied to infected areas, swiftly healing diseased corals while preventing drug leakage into the environment. The design was optimized to ensure monodirectional drug release to the infected coral tissue within 1 week of treatment, addressing the infected coral tissue and preventing environmental release. This technology successfully inhibited *in vitro* growth of *Vibrio coralliilyticus* and halted the progression of tissue-necrosis-like symptoms in 90% of aquarium corals tested, serving as a milestone for future developments and applications.

INTRODUCTION

Corals are marine invertebrates functioning as holobionts, engaging in complex symbiotic relationships. They produce calcium carbonate to form their exoskeletons, which in turn build coral reefs, some of the most biodiverse ecosystems in the world. These coral holobiont hosts several symbiotic microorganisms, such as dinoflagellate algae (primarily from the Symbiodiniaceae family) and bacteria,[1] archaea, fungi, and viruses, with dinoflagellates and bacteria representing a significant component of the coral microbiome and playing an essential role in maintaining holobiont homeostasis.[2] Symbiotic bacteria play a role in regulating coral responses to thermal or oxidative stress, with their distribution and community composition varying depending on the bacterial species involved.[3,4] However, not all symbiotic bacteria have solely beneficial effects on

Please cite this article in press as: Scribano et al., Eco-friendly active film and sealant for underwater drug delivery to diseased corals, One Earth (2025), https://doi.org/10.1016/j.oneear.2025.101356

corals; some can induce harmful disease, and others, such as opportunistic strains, can leverage favorable community dynamics to thrive and disrupt the holobiont equilibrium.[5–9]

In recent years, the spread of coral diseases has drastically increased, and it is estimated that by 2100 nearly 80% of corals will be infected.[10] This often happens because the corals' ability to withstand specific pathogen attacks and general stressors is closely tied to their health status (e.g., healthy vs. bleached),[11] whereby the rise in sea temperature and the decline in seawater quality weaken corals, making them more susceptible to outbreaks.[10]

Coral-pathogen interactions occur through either biotic or abiotic vectors such as coral predators (e.g., *Drupella* sp.), water currents and sediment movements,[12] sludge spilling,[13] and plastic pollutants.[14,15] Coral pathogens include bacteria but also fungi and viruses.[16–18] Coral diseases are challenging to distinguish due to their symptom similarity and the non-uniform nomenclature. Moreover, among all the 40 identified coral diseases, the etiopathogenic agent has been identified only in a few of them, further complicating their eventual treatment.[13,19] Such complexity in etiopathology identification mainly relies on the identification of the entire microbial community present in the coral during the disease, as some of the diseases, such as the black band disease (BBD), seem to be caused by a consortium of microorganisms rather than a single infecting agent.[20] Other diseases such as the skeletal eroding band (SEB) and brown band disease (BrB), which are widely distributed in the Indo-Pacific area, seem to be caused by ciliated protozoa.[13,19] Another example is the pathogen of the stony coral tissue loss disease (SCTLD), an aggressively spreading disease that has affected most Caribbean reefs, which is still unknown and/or not confirmed.[21,22] Outbreaks can even occur in coral nurseries or aquaria deputed to hobbyist businesses, despite these environments being more protected by water-filtration systems and sterilization through UV light. Here, corals are protected for exhibition or cultivated and grown before their transplantation into the reef. For instance, in the context of aquaculture for reef restoration, a disease outbreak in the closed-system nurseries could cause the loss of a significant number of colonies and impact restoration efforts.[23] Rapid tissue necrosis (RTN) disease is often found in aquaria and is associated with *Vibrio harveyi*.[24] This disease is characterized by a quick tissue detachment from the coral skeleton, which may cause the death of the coral within 24 h of the appearance of the lesion.[24]

Currently, a few options to treat such infections have been proposed, involving mechanical removal of the lesion (infected coral tissue) or administration of probiotics, phage therapy, or active molecules,[25–28] but these methods present drawbacks that limit their effectiveness. For instance, mechanical separation of the infected site from the healthy coral may produce new lesions and entry points for other pathogens present in the surrounding environment, favoring the reinfection of the coral.[26] While administering probiotics is promising for preventing coral diseases in laboratory settings, it presents challenges in real-world scenarios. Probiotics are specific to particular coral species, and the potential unpredictable effects on the local marine bacterial community still need to be understood.[27] Phage administration is a ready-to-use method to attack a pathogenic agent causing a specific infection. However, the high specificity of this technique and the lack of information regarding the etiopathology of many coral diseases make this approach inefficient for use on uncharacterized diseases.[29] Finally, active molecules, such as antibiotics, which are massively available and possess a broad spectrum of action, could be a straightforward solution for coral diseases. However, there are concerns regarding the development of antibiotic resistance, the alteration of the holobiont community, and potential cascading effects such as dysbiosis and the spread of opportunistic pathogens.[30]

In the wild, antibiotics are usually directly applied to the coral infection site via topical pastes.[25,31–34] However, antibiotic molecules can be entrapped in the hydrophobic and/or highly networked matrix, such as silicon-based and epoxy-resin-based materials. Moreover, they are applied as a single, uniform, and continuous layer directly onto the infected area, ensuring its coverage. The parameters influencing drug diffusion from a matrix, including dissolution into the environment, are noteworthy as they involve Fick's laws (concentration and dispersion), the hydrophobic/hydrophilic properties of the material, crosslinking, and other water-related parameters such as swelling, erosion, temperature, pH, and ionic strength.[35–37] Among them, the quantity of water in contact with the material plays a crucial role in drug diffusion and the linked phenomenon of matrix erosion, especially when a material is applied as a monolayer on corals.[38] Indeed, at the interface between the coral tissue/infected area and the active material surface, a very low amount of water will be present, especially compared to the quantity of water in the sea. The difference in volume between the two exposed sides of the monolayered paste could represent an obstacle to the diffusion of the drug toward the infected coral site, reducing efficacy and, thus, potentially inhibiting the efficacy of the treatment.[39–41] Indeed, at the interface between the active material and the external marine environment, the drug diffusion and the erosion of the matrix mediated by seawater are theoretically enhanced compared to the internal interface. This difference may favor the diffusion of the antibiotic in the environment.[30,31] Approaches like this one can foster the previously described concerns regarding the use of antibiotics.[42–45]

In the past, similar challenges faced in treating human infections have been resolved through the dedicated design of topical drug-delivery systems. These deliver antibiotics directly to the infected area, ensuring drug availability at the proper concentrations throughout the treatment period. The constant and localized administration enhances the overall healing rate while minimizing interaction with non-involved tissue.[40,46] Inspired by the principles for the design of buccal delivery systems to treat human infection in wet environments, we developed a new strategy to treat coral disease. Specifically, in buccal infections, the delivery system releases the drug unidirectionally by having a hydrophilic layer loaded with the drug that comes into contact with the buccal tissue (both infected or healthy), and a covering hydrophobic external layer to avoid the dispersion of the drug in the external wet environment comprising the mouth, saliva, sublingual area, and so forth.[47] This scenario is rather similar to the coral infection case. Hence, an ideal underwater drug-delivery system should focus its intervention on the infected region, focusing the drug delivery on one single spot and avoiding the dispersion of drugs into the surrounding environment.[47,48] Moreover, the ideal system should present suitable mechanical

Please cite this article in press as: Scribano et al., Eco-friendly active film and sealant for underwater drug delivery to diseased corals, One Earth (2025), https://doi.org/10.1016/j.oneear.2025.101356

CellPress
OPEN ACCESS

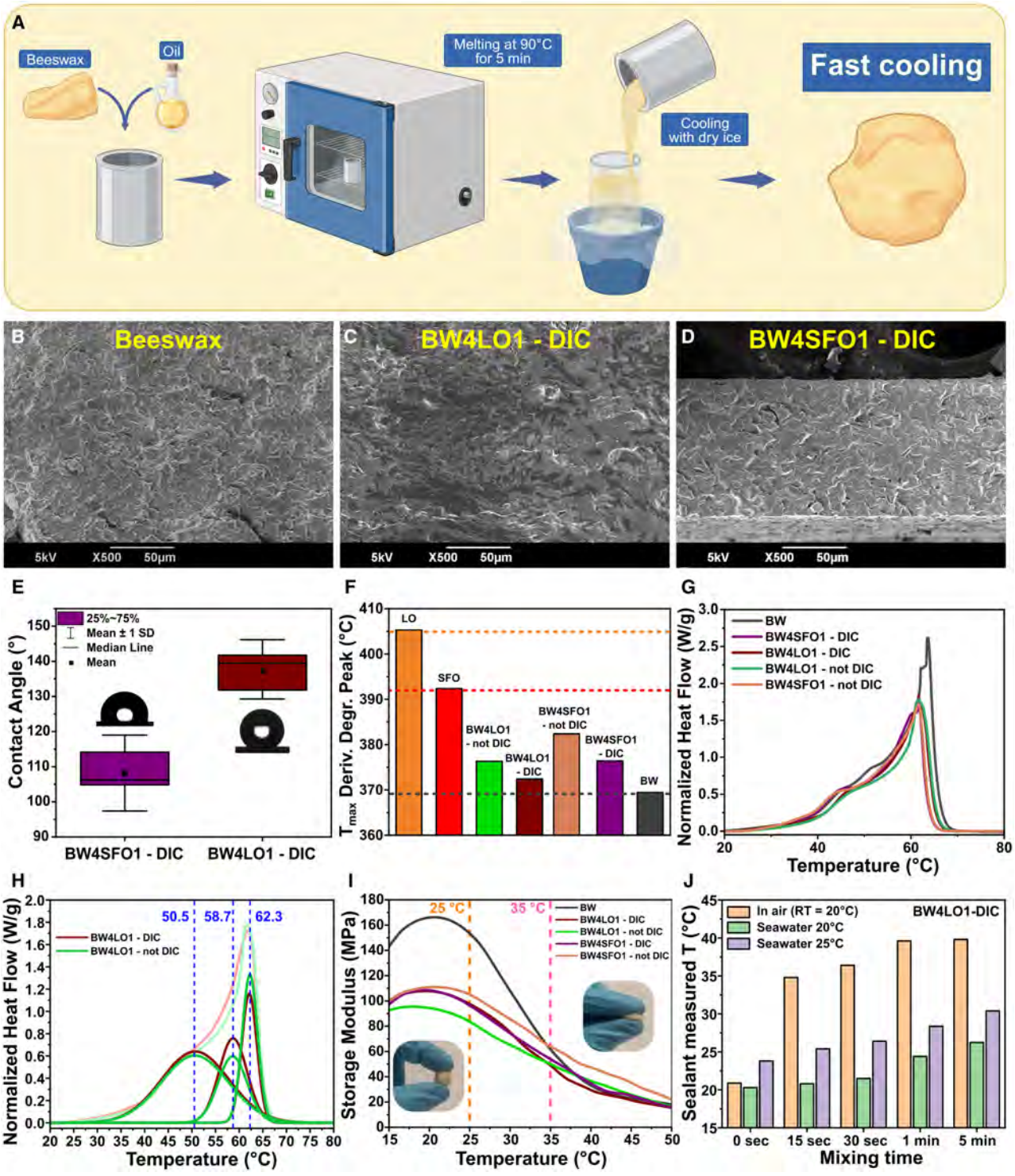

Figure 1. Sealant characterization

(A) Schematic representation of the sealant preparation.

(B–D) SEM images of BW (B), BW4LO1-DIC (C), and BW4SFO1-DIC (D) sealants.

(E) Water contact angle of the sealants BW4LO1-DIC and BW4SFO1-DIC, the results are expressed as mean, median, SD; the insets are images representative of the shape of water droplets on the material surface.

(F) Temperatures at which each sample tested loses most of its mass in TGA; dotted horizontal lines represent the temperature degradation of the reagents LO, SFO, and BW.

(G) First melting round (endo up) of DSC of BW, BW4SFO1-DIC, BW4LO1-DIC, BW4SFO1-not DIC, and BW4LO1-not DIC.

(legend continued on next page)

Please cite this article in press as: Scribano et al., Eco-friendly active film and sealant for underwater drug delivery to diseased corals, One Earth (2025), https://doi.org/10.1016/j.oneear.2025.101356

properties such as flexibility, moldability, and adhesivity as well as being user-friendly.[49] Finally, the underwater drug-delivery system should promote coral tissue growth, and its dispersion in the environment should not damage the environment itself.[48,50]

Recently, Contardi et al. proposed the first *in situ* drug-delivery system for coral wounds, using a hydrophilic polymeric film to deliver antiseptics to the wounded site and a sealing thermoplastic to separate the covered wound from the surroundings, leading the way to underwater coral drug delivery.[48] However, the effectiveness of the proposed system as a unidirectional drug-delivery system on diseased coral was not proven. Moreover, the thermoplastic sealant needed to be melted just before application, which could be problematic in an *in situ* setting.

Here we propose a new, improved, two-component system for treating infected corals based on the sequential application of a hydrophilic drug-loaded film and a bio-based hydrophobic sealant at the diseased site. The film is applied to the coral infection and, subsequently, the area is isolated with the sealant. This approach allowed for unidirectional drug release, preventing dispersion in the surrounding environment and potentially contributing to antibiotic resistance. Moreover, the treatment demonstrated its efficacy against *Vibrio coralliilyticus in vitro* and against a tissue-necrosis-like disease *in vivo*. This approach sets the basis for a new conceptualization of underwater drug delivery and may potentially inspire new tools for the treatment of coral diseases.

RESULTS

Methods summary

In this study, we present a two-component system for treating diseased corals and preserving the surrounding environment. Our approach involves the application of a hydrophilic, antibiotic-loaded film directly onto the diseased site of the coral, covered by a natural hydrophobic paste-like sealant, to ensure that the drug is released exclusively toward the coral. The hydrophilic films were made of chitosan (C), a natural polymer present in the exoskeleton of crustaceans,[51] and polyvinylpyrrolidone (P), a biodegradable and hydrophilic polymer commonly employed in the pharmaceutical field.[50,52,53] These materials were primarily selected for their capacity to form free-standing films and for being biodegradable. The antibiotics loaded in the films were two wide-spectrum antibiotics, ciprofloxacin (Cipro) and gentamicin sulfate (Gent), both previously tested against coral pathogens as *V. coralliilyticus*.[44] The sealants were prepared by melting and mixing the natural thermoplastic beeswax (BW) and two different types of oils, sunflower oil (SFO) or linseed oil (LO), which mostly differ in the amount of unsaturated fatty acid in their composition. A dry ice cooling method was used to better entrap the oil in the BW matrix and to optimize its thermo-responsivity. Films based on different weight ratios of P and C, and sealants composed of BW and different plant-based oils, were characterized and compared in terms of morphological, chemical, thermal, mechanical, and water-stability properties to study their performance under thermal and mechanical stress and their interaction with the marine environment. Finally, the unidirectional drug delivery of the (film + sealant) system toward the infected coral site was investigated, and its efficacy was evaluated both *in vitro* against *V. coralliilyticus* and *in vivo* against the tissue-necrosis-like disease. All the acronyms used in this study are summarized in Table S1.

Characterization of the sealants

The preparation of the natural BW/plant-based sealant is schematically represented in Figure 1A and analytically described in the methods section. In brief, the BW, which was selected for its capacity of being moldable at relatively low temperatures, was melted in the presence of the oil (either LO or SFO) in a ratio of 4:1, mixed, and quickly cooled through the dry ice cooling method to improve oil miscibility in the BW matrix. Four sealants were prepared and named, based on their material and ratio composition and their production method, as BW4LO1-DIC (dry ice cooled), BW4LO1-not DIC, BW4SFO1-DIC, and BW4SFO1-not DIC. The sealants were tested to evaluate differences among composition, production methods, and overall performances. The obtained plant-based pastes had a yellowish color, similar to the pristine BW, and were morphologically characterized using scanning electron microscopy (SEM). This technique allows the user to obtain 2D high-contrast images of the surface material morphology, a key feature that affects the material properties, such as mechanical and degradability properties.[54,55] Sealants with LO (BW4LO1 in Figure 1C) presented an inhomogeneous surface with differentiated zones, different from those present in the sealants with SFO (BW4SFO1 in Figure 1D), which seemed more homogeneous and similar to the pristine BW (Figure 1B).

Water contact angle (WCA) analysis was performed to evaluate the hydrophobicity nature of the material surface, essential information for understanding the interaction between the materials and the water.[49] The mean WCA values of the sealants were measured. The samples BW4SFO1-DIC, BW4LO1-DIC, BW4SFO1-not DIC, and BW4LO1-not DIC (Figures 1E and S1A) presented a mean WCA of 108.2°, 137.7°, 133.1°, and 134.5°, respectively, indicating that the surfaces of all the sealants appeared hydrophobic. Hydrophobicity is a necessary requirement to act as a shield against the seawater and avoid the spread of the drug from the internal film toward the environment. Fourier transform infrared (FTIR) spectroscopy analysis showed no variation in the chemical functional groups of the individual components after the fabrication process (Figure S1B), indicating that no chemical interaction occurred between the BW matrix and the oil.[56]

(H) Deconvolved curves of DSC first melting round (endo up) of BW4LO1-DIC and BW4LO1-not DIC; dashed lines indicate the temperature at which the deconvoluted curves have their peak center.
(I) Mechanical dynamical transition of the storage modulus relative to temperature variations of BW and the four pastes; insets are a visual representation of the hardness of the sealant produced.
(J) BW4LO1-DIC sealant temperature at different time points upon hand mixing in air and seawater environment (RT, room temperature).
See also Figure S1; Tables 1 and S2.

Please cite this article in press as: Scribano et al., Eco-friendly active film and sealant for underwater drug delivery to diseased corals, One Earth (2025), https://doi.org/10.1016/j.oneear.2025.101356

Table 1. Areas of the peaks of the first melting round deconvolved curves

Sample name	Peak at 50.5°C	Peak at 58.7°C	Peak at 62.3°C
BW4LO1-DIC	11.48	5.65	4.66
BW4LO1-not DIC	10.72	4.58	5.45

The enthalpy (area under the curve, measured as J/g) of the peaks of the first melting round deconvolved curves obtained by the residuals first derivative method.

Thermal stability properties of the materials were investigated by thermogravimetric analysis (TGA) and differential scanning calorimetry (DSC) analysis. TGA gives information on the stability of the materials at increasing temperatures expressed as a weight loss.[57] The first derivative TGA curves showed that the main degradation peaks of BW4LO1-DIC and BW4SFO1-DIC sealants (Figures S1C, S1D, and 1F) occurred between those of the respective oil and the BW. Specifically, the main weight loss for BW was observed at 369.4°C, for LO at 405.3°C, and for SFO at 392.4°C, whereas BW4LO1-DIC and BW4SFO1-DIC showed the main degradation peak at 372.4°C and 376.4°C, respectively. The samples that did not undergo the dry ice cooling, BW4LO1-not DIC and BW4SFO1-not DIC, showed the main degradation peak at 376.3°C and 382.4°C, respectively, indicating a different type of interaction between the BW and the oils compared to sealants that underwent dry ice cooling.

To further investigate the internal structure and distribution of the various components in sealants with different compositions and preparation methods, DSC analyses were performed, the main results of which are shown in Figures 1G, 1H, and S1E. In DSC analysis, the materials undergo a thermal ramp, and the instruments detect heat capacity of absorbing (exothermic peaks) and releasing (endothermic peaks) heat from the environment. This fundamental information allows investigation of the physical changes in the materials under thermal stress, such as crystallinity, amorphous degree, and glass-transition temperature. The area under the curve of the first melting cycle of BW was 27.85, whereas those for BW4SFO1-DIC, BW4SFO1-not DIC, BW4LO1-DIC, and BW4LO1-not DIC were respectively 21.49, 22.01, 21.53, and 20.50. As the sealants' areas are smaller than the BW's area, it is reasonable to assume that the oils lowered the energy necessary for the melting of the pastes. In addition, using the deconvolution method on the sealants' first melting round, it was also possible to highlight the differences in the preparation methods between BW4LO1-DIC and BW4LO1-not DIC and between BW4SFO1-DIC and BW4SFO1-not DIC (Figures 1H and S1E). Based on the areas under the deconvolved peaks detected (Figure 1H and Table 1), it was observed that higher energy was required to melt the semi-crystalline structures formed in BW4LO1-DIC at 50.5°C and 58.7°C compared to BW4LO1-not DIC. The opposite trend was found for the third peak at 62.3°C. The same pattern was noticed on comparing the deconvolution of BW4SFO1-DIC and BW4SFO1-not DIC (Figure S1E and Table S2). Here, BW4SFO1-DIC samples presented a larger area, corresponding to higher enthalpy, than BW4SFO1-not DIC samples in the first three deconvoluted peaks at 48.1°C, 56.6°C, and 60.3°C. However, the trend was inverted in the fourth peak at 61.9°C. This behavior could be attributed to the different cooling times upon preparation. In the "not DIC" samples, the slower cooling allowed for the formation of fewer crystal nucleation points and the growth of the pre-existing crystals, thus leading to a less homogeneous oil distribution with larger crystals that need higher temperatures to melt.

Reef-building corals are typically found in waters where temperatures range from approximately 25°C to 30°C, with minimal seasonal variation, but they are also present in areas with more extreme temperatures ranging between 15°C and 36°C.[58,59] Next, the sealants' mechanical characteristics were evaluated at various temperatures to identify the best candidate for use in real conditions. To this end, loss and storage modulus differences over the expected usage temperature range were analyzed using dynamic mechanical thermal analysis (DMTA).[49] In Figure 1I, the storage modulus of the different pastes is represented as a function of the temperature. BW4LO1-DIC presented a maximum storage modulus of 108.0 MPa at 19.4°C, BW4LO1-not DIC showed a peak of 95.7 MPa at 18.0°C, BW4SFO1-DIC had a maximum of 84.2 MPa at 17.2°C, and BW4SFO1-not DIC had a maximum of 111.3 MPa at 20.7°C. In contrast, the pristine BW had a larger storage modulus of 166.7 MPa at 20.5°C, making it harder compared to the sealants within the range from 15°C to 25°C. From 25°C to 35°C, a general decrease in the storage modulus was observed for all samples, indicating a softening of the sealants. Specifically, at 30°C, BW decreased its storage modulus to 108.1 MPa, and at 35°C the modulus value was 61.7 MPa. Similarly, for BW4LO1-DIC, BW4LO1-not DIC, BW4SFO1-DIC, and BW4SFO1-not DIC, the hardness of the sealants was 75.3, 65.3, 74.4, and 85.6 MPa at 30°C and decreased to 48.9, 50.0, 54.0, and 64.0 MPa at 35°C, respectively. Therefore, around 20°C, the sealants showed the highest stiffness. From 24°C, they start reducing their modulus and become softer at around 30°C, producing a suitable mechanical thermo-responsivity crucial for their application on corals.

In Figure S1F, the tan(δ) value of BW and the pastes is plotted as a function of the temperature. BW's glass transition temperature (T_g) was 20.5°C, whereas the T_g values for BW4LO1-DIC and BW4LO1-not DIC, identified as the highest peak in the curves, were 19.4°C and 17.5°C, respectively. BW4SFO1-DIC and BW4SFO1-not DIC did not present a clear transition peak at the range considered. A lower T_g in the sealants could be attributed to the presence of the different oils. Overall, the results obtained in the TGA, DSC, and DMTA analyses for the sealants demonstrated that the dry ice cooling treatment improved the dispersion of the oils in the BW matrix and increased the responsiveness of the samples to temperature-induced mechanical transitions, compared to the not-DIC sealants and the BW. In addition, the sealant BW4LO1-DIC resulted in being the softest at 35°C, had the highest decrease in loss of storage modulus among the sealants from 25°C to 35°C (around 49.9%, see Figure S1G) and presented the most hydrophobic behavior. For these reasons, it was selected to perform the subsequent experiments and evaluate the performance of the two-component system on corals.

For practical application on corals, the sealant is intended to be hand mixed and warmed to approximately 35°C (human skin temperature) underwater before being applied to tropical corals at seawater temperatures of around 25°C. To simulate

Please cite this article in press as: Scribano et al., Eco-friendly active film and sealant for underwater drug delivery to diseased corals, One Earth (2025), https://doi.org/10.1016/j.oneear.2025.101356

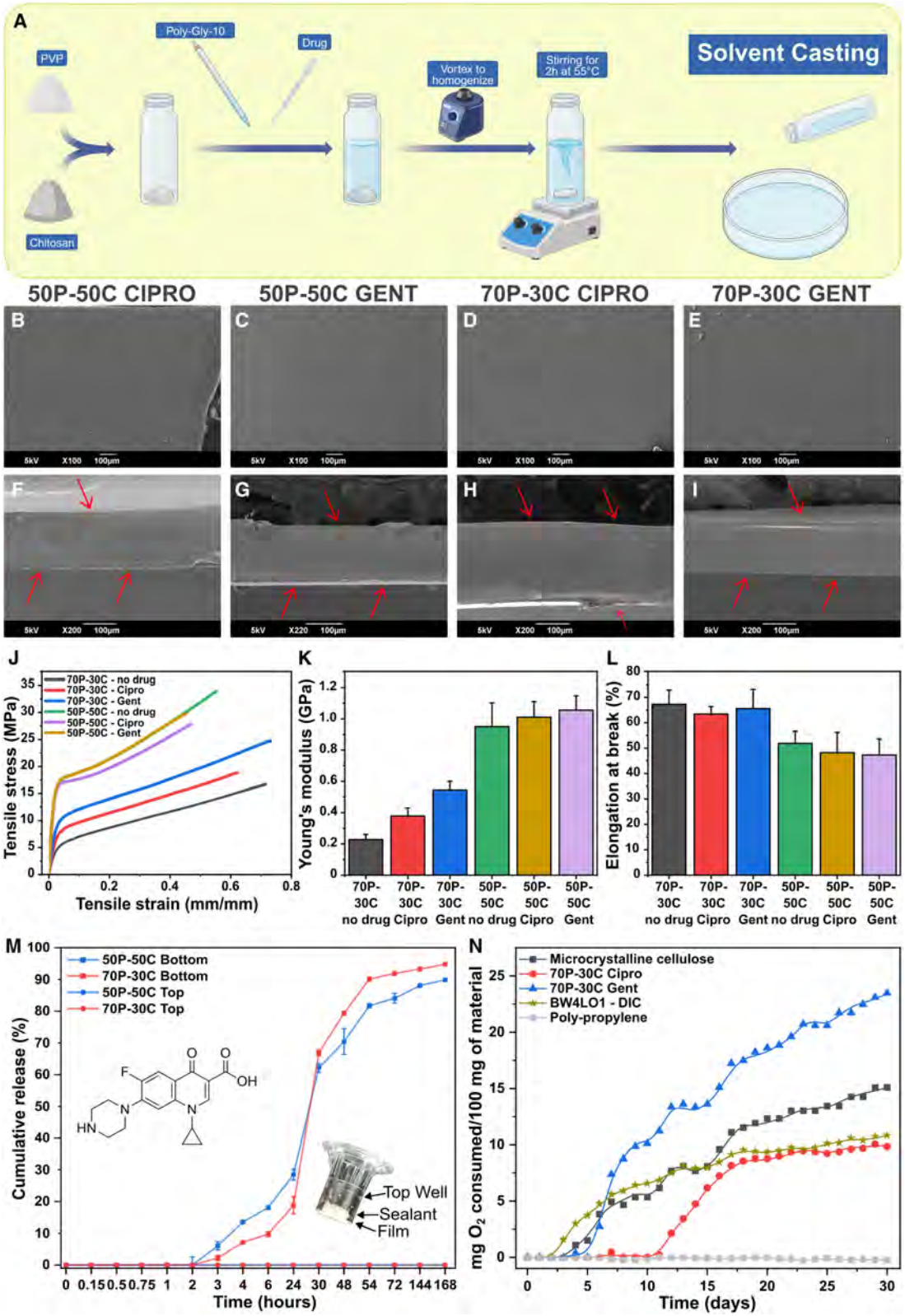

Figure 2. Films and two-component system characterization

(A) Schematic representation of the films' production.

(B–E) Top-view SEM images of 50P-50C-Cipro (B), 50P-50C-Gent (C), 70P-30C-Cipro (D), and 70P-30C-Gent (E) films.

(legend continued on next page)

Please cite this article in press as: Scribano et al., Eco-friendly active film and sealant for underwater drug delivery to diseased corals, One Earth (2025), https://doi.org/10.1016/j.oneear.2025.101356

the real-world application, a test on the effective internal temperature of the paste after hand mixing using a thermocouple was performed.[60] The sealant BW4LO1-DIC was hand mixed in the air at room temperature (20°C) and in seawater at two different temperatures, 20°C and 25°C, and the internal temperature was monitored at different time points (Figure 1J). The highest temperature variation upon mixing in air was obtained after 1 min of hand mixing, with the internal temperature reaching 39.8°C. In seawater at 20°C, the internal sealant temperature reached a maximum of 27.2°C after 5 min of mixing. In seawater at 25°C, the sealant reached a maximum of 30.8°C after 5 min of underwater mixing. BW4LO1-DIC became soft enough to be molded by the user both in air and seawater.

Characterization of the drug-loaded films

Films with different proportions of P and C (50:50 and 70:30, Figure S2A), with polyglycerol-10 as a plasticizer, and loaded with either Cipro or Gent, were produced using the solvent casting method,[57,61] and their preparation is schematically described in Figure 2A. Films were named based on their polymeric composition and on the type of loaded antibiotic, as 50P-50C-no drug, 50P-50C-Cipro, 50P-50C-Gent, 70P-30C-no drug, 70P-30C-Cipro, and 70P-30C-Gent. The films appeared optically transparent (see Figure S2A), and their microscopic morphology, investigated by SEM, revealed homogeneity, both on the surface and in the cross-section, independently of the polymer ratio or the loaded drug (Figures 2B–2I and S2B). This suggests that the two drugs were well dispersed in the polymer matrices.[62] The films were also chemically analyzed using FTIR spectroscopy to detect chemical interactions among the polymers and the drug, and all the acquired spectra are reported in Figure S3A. FTIR spectroscopy analysis of the films' spectra mainly showed the polymers' contribution. In particular, the typical alcohol (C-*O*-H) and ether (C-*O*-C) stretching modes of C were observable in the region between 1,150 and 950 cm^{-1}, where it overlaps with the polyglycerol-10, which presents similar vibration modes (Figure S3A). The most evident peak for P was at 1,652 cm^{-1}, which is attributed to the carbonyl (C=O) stretching mode. Finally, the peaks of the drugs are not visible, most likely due to their low amount in the films (1% [w/w]) and because they are covered by the polymer's vibration peaks.[63]

Regarding the mechanical properties, the higher the C content in the films, the greater their Young's modulus and the lower their stretchability (Figure 2J). This was measured with a tensile stress analysis, which is used for the evaluation of the elasticity and tensile strength of the materials.[64,65] In particular, the films with a weight proportion of 50P-50C had mean Young's moduli of 0.95 GPa for 50P-50C-no drug, 1.01 GPa for 50P-50C-Cipro, and 1.05 GPa for 50P-50C-Gent, being from 2- to almost 5-fold higher than the 70P-30C films (Figure 2K). Indeed, these latter presented mean Young's moduli of 0.23 GPa for 70P-30C-no drug, 0.38 GPa for 70P-30C-Cipro, and 0.54 GPa for 70P-30C-Gent, confirming the role of the C content in the films. Interestingly, the drug loaded in the films seems to increase their Young's moduli compared to the films with no drug loaded, with Gent-loaded films having the highest values. This trend is inverted for the elongation at break (Figure 2L). The 70P-30C films, both loaded with drugs and without drugs, showed higher elongation than the 50P-50C-based films. Specifically, for the 70P-30C films with and without drugs, the elongation at break was around 65%, whereas for the 50P-50C films, the values were about 50%, suggesting that this feature was not affected by the presence of the two drugs. The tensile stress at maximum load (Figure S3B) was smaller for the 70P-30C films than for the 50P-50C counterparts. In particular, the 70P-30C-no drug, 70P-30C-Cipro, and 70P-30C-Gent had a mean tensile stress of 19.05 MPa, 17.95 MPa, and 24.47 MPa, respectively. 50P-50C-Cipro had a mean value of 25.71 MPa and 50P-50C-Gent of 28.46 MPa, and 50P-50C-no drug showed the highest tensile stress at a maximum load of 30.83 MPa. Despite the differences in Young's modulus and tensile stress at maximum load among the films, the composition did not drastically influence the overall capacity of being stretched and elongated. The film's stretchability is a functional property for its efficient wrapping around the coral branches with the infected sites (see Figure S2A). Therefore, we selected the 70P-30C films to perform the *in vivo* tests.

The dynamic water contact angle (DWCA) was acquired to observe the interaction between the surface of the films and the seawater for the first 5 min after their contact,[66] and the results are shown in Figure S3C. Teflon was used as an inert surface for comparison reasons and had a WCA of 102°, which remained practically stable during the 5 min of the measurement, while the drop volume did not undergo any significant variation. Instead, while the films showed an initial WCA between 105° and 95°, after a few seconds, the WCA started decreasing due to the strong hygroscopic nature of the films toward water, resulting in the complete absorption of the deposited seawater drops within 30 s. Indeed, P and C are well-known hygroscopic polymers with high swelling capability.[67,68] Hygroscopicity of the material is directly correlated with the drug-release kinetics of the film in watery environments.[69] In particular, a higher hygroscopicity is correlated with a faster drug release, which is a requested feature to promptly act against the bacterial infection.[70]

(F–I) Cross-section SEM images of 50P-50C-Cipro (F), 50P-50C-Gent (G), 70P-30C-Cipro (H), and 70P-30C-Gent (I) films; red arrows indicate the extremities of the films.

(J) Stress-strain curves of the films' mechanical tensile stress/strain.

(K) Mean Young's modulus and relative standard deviation of the films.

(L) Mean elongation at break and relative standard deviation of the films.

(M) Cumulative release of Cipro from the transwell model for the 50P-50C-Cipro (blue lines) and 70P-30C-Cipro (red lines) films in the top and bottom wells (circles and squares, respectively); the results are expressed as mean and SD; the inset shows a photo of the transwell setup.

(N) Biochemical degradation activity within 30 days of 70P-30C-Cipro, 70P-30C-Gent, and BW4LO1-DIC, and microcrystalline cellulose and polypropylene as references.

See also Figures S2 and S3.

Please cite this article in press as: Scribano et al., Eco-friendly active film and sealant for underwater drug delivery to diseased corals, One Earth (2025), https://doi.org/10.1016/j.oneear.2025.101356

Table 2. Minimal inhibitory concentration

Tested drug		MIC (μg/mL)									
		0.125	0.25	0.5	1.0	2.0	4.0	8.0	16.0	32.0	64.0
Ciprofloxacin	interpretative category	R	I	S	S	S	S	S	S	S	S
Gentamicin	interpretative category	R	R	R	R	R	R	R	I	S	S

Concentrations of the drug were tested on *V. coralliilyticus*. R, resistant; I, intermediate; S, susceptible to the drug dose administered.

Two-component system drug release and biodegradability

To maximize the efficacy of the antibiotics embedded in the films and avoid their release in the environment, the performance of the two-component system (film + sealant) in directing the drugs exclusively toward the infected coral site was investigated. A transwell system was used to simulate the two-component system placed onto the infected coral site at its interface with the sea. The film and the paste were placed within the transwell insert, as shown in the scheme in Figure S3D. This produced a separate compartment in the inner top part of the insert, as shown in Figure 2M, thus preventing seawater diffusion between the top and the bottom compartments.

In the experimental setup, the top well of the transwell represents the external marine environment, while the bottom well simulates the coral-infected site. The film is in contact with the bottom well and the sealant with the upper well, with the film and sealant also in contact with each other. The results of the Cipro diffusion in both compartments over 168 h (7 days) are shown in Figure 2M. In both the 70P-30C and 50P-50C samples, Cipro started reaching the bottom compartment after 2–3 h; more than 60% of the drug was released within the first 24–30 h and slowly continued to diffuse until the 6th day. Minimal differences between the samples were observed in the first 24 h, when the samples with a higher amount of C had an initial faster release, probably due to the higher capacity of C to swell compared to P. On the contrary, no diffusion of Cipro was detected during the experiment in the top compartment, confirming the excellent sealing properties of BW4LO1-DIC.

One of our goals was to be minimally invasive to the corals and marine environment, avoiding the introduction of non-biodegradable components. To confirm this, the biodegradability of the films, with and without the drugs, and of the sealant was tested using biochemical oxygen demand (BOD), the results of which are shown in Figures 2N and S3E. In this test, the materials were kept in seawater for 30 days, and the consumption of oxygen was directly related to the materials' degradation (ISO 23977-2: 2020). Microcrystalline cellulose (positive control) and polypropylene (negative control) were also tested, showing oxygen consumption of 15.1 and 0.0 mg O_2/100 mg of material, respectively. After 3 days, the BW4LO1-DIC sample started degrading, obtaining a final oxygen consumption of 10.8 mg O_2/100 mg of material. All the films were biodegradable, producing values between 7.4 and 23.5 mg O_2/100 mg of material (Figures 2N and S3E).

Antibacterial properties

Minimal inhibitory concentration (MIC) is an assay where different concentrations of antibiotic are added to a specified amount of bacteria to define the minimal concentration of drug necessary to inhibit the growth of the microorganisms.[71] The MIC of Cipro and Gent against *V. coralliilyticus* was evaluated by measuring the optical density (OD) of the growth medium after 24 h in the presence of different concentrations of antibiotics compared to untreated samples to ensure that the effective amount of drug was loaded in the films. As shown in Table 2, the susceptibility of *V. coralliilyticus* for Cipro was higher than for Gent, resulting in MIC values of 0.5 and 32.0 μg/mL, respectively. Antibacterial growth tests were then performed to further correlate the drugs' antibacterial capacity and their release from the produced films.

A disk-diffusion assay was performed using films instead of standard paper disks.[61,62] Figure 3A shows the plates with the different areas of *V. coralliilyticus* growth inhibition determined by the drug diffusion from the films in the agarized growth medium. The mean diameters of growth inhibition are presented in Figure 3B. All the investigated films showed a higher antibacterial effect compared to the control samples. To confirm this outcome, statistical analysis was performed among the different experimental groups (positive control, 70P-30C-Gent, 50P-50C-Gent, 70P-30C-Cipro, and 50P-50C-Cipro). The overall one-way ANOVA performed presented statistical significance (overall $p < 0.001$). In particular, almost all the interactions tested using a Bonferroni post hoc test were significant ($p < 0.05$). A significant difference in the inhibition growth diameter was obtained for all the films when compared with the control. The only interaction that did not show significance was between the films containing Gent, which presented similar inhibition diameters of 14.8 and 15.0 mm (for the 70P-30C and 50P-50C, respectively). The difference between the inhibition area of the 50P-50C-Cipro and the 70P-30C-Cipro film disks, with an inhibition diameter of 26.2 mm and 22.4 mm, respectively, instead presented a significant statistic ($p < 0.05$). These results may be attributed to a probable synergistic effect between C and Cipro.[62]

The growth inhibition of *V. coralliilyticus* in a liquid medium condition within 24 h was evaluated to further describe the antibacterial action of the films and the proper diffusion and efficacy of the antibiotics against the bacterium. Three different film concentrations (1.0, 2.5, and 5.0 mg/mL) per film type (70P-30C-Gent, 50P-50C-Gent, 70P-30C-Cipro, and 50P-50C-Cipro) were tested, the results of which are reported in Figure 3C.[61] An inert film of Teflon and a medium without any film were also used as a negative control. *V. coralliilyticus* was inoculated at a concentration of $\sim 10^6$ colony-forming units (CFU) in all the wells as a T_0, and the final concentration of bacteria was evaluated after 24 h ($\sim 10^9$ CFU).

Two-way ANOVA was run among the negative controls and the films in all conditions (polymeric compositions, loaded antibiotics, and concentrations) and all their interactions. The test resulted in a statistically significant result with a p value of <0.001.

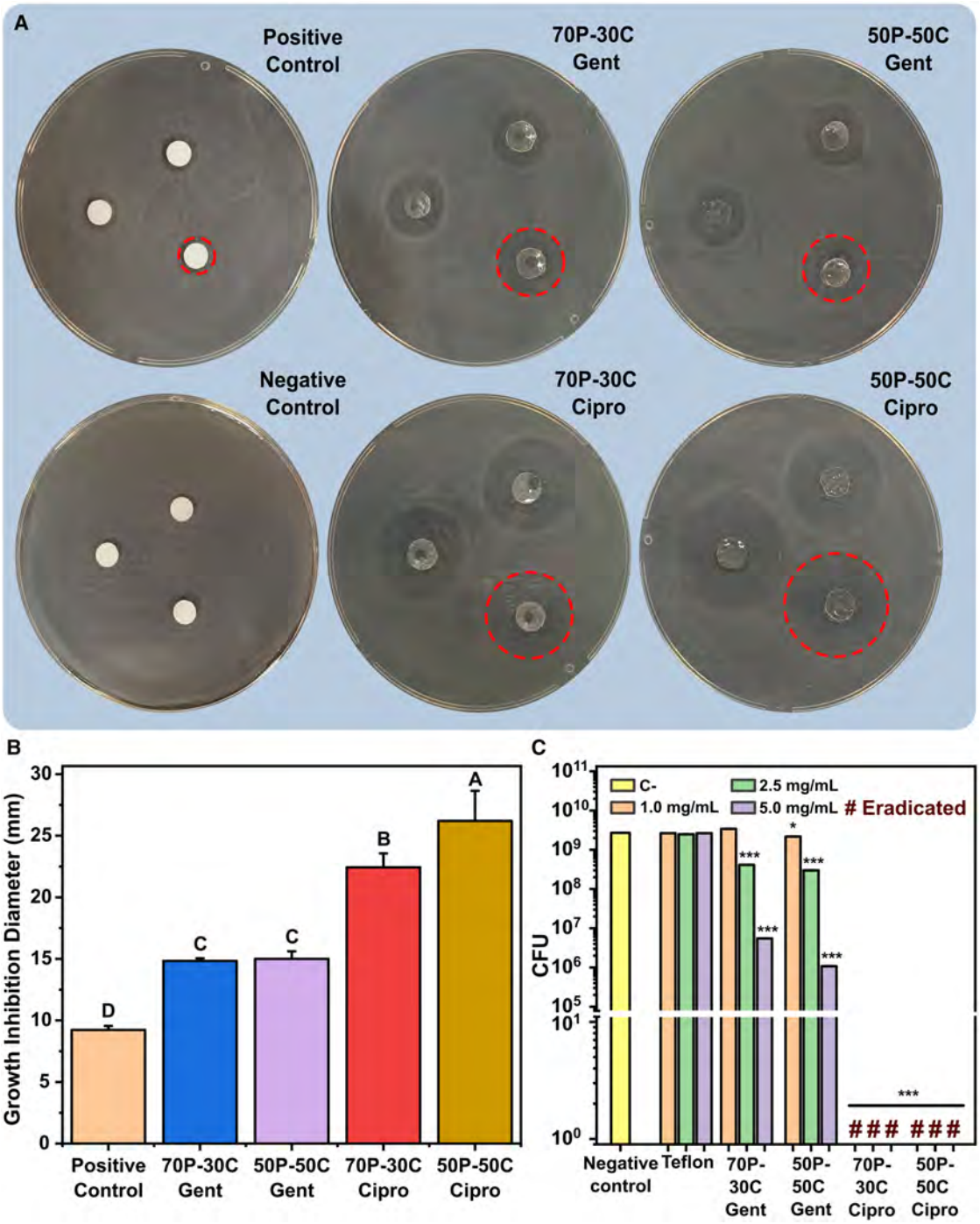

Figure 3. Antibacterial properties

(A) Photographs of Petri dishes used in the disk-diffusion assay with *V. coralliilyticus* of the positive control, 70P-30C-Gent, 50P-50C-Gent, negative control, 70P-30C-Cipro, and 50P-50C-Cipro samples; red dotted rings indicate the inhibition growth ring on the different plates.

(B) Mean maximum diameter and relative standard deviation of the disk-diffusion assay for positive control, 70P-30C-Cipro, 70P-30C-Gent, 50P-50C-Cipro, and 50P-50C-Gent. One-way ANOVA followed by Bonferroni post hoc test: different letters on top of the histogram indicate significance ($p < 0.05$) among groups.

(C) Bactericidal effect of the films in the marine broth medium inoculated with *V. coralliilyticus*. The results are expressed as mean and SD. The hash mark (#) indicates that the bacterium was fully eradicated. Two-way ANOVA followed by Bonferroni post hoc test: antibacterial efficacy is highlighted as $^{*}p < 0.05$, $^{**}p < 0.01$, and $^{***}p < 0.001$.

See also Table S3.

Please cite this article in press as: Scribano et al., Eco-friendly active film and sealant for underwater drug delivery to diseased corals, One Earth (2025), https://doi.org/10.1016/j.oneear.2025.101356

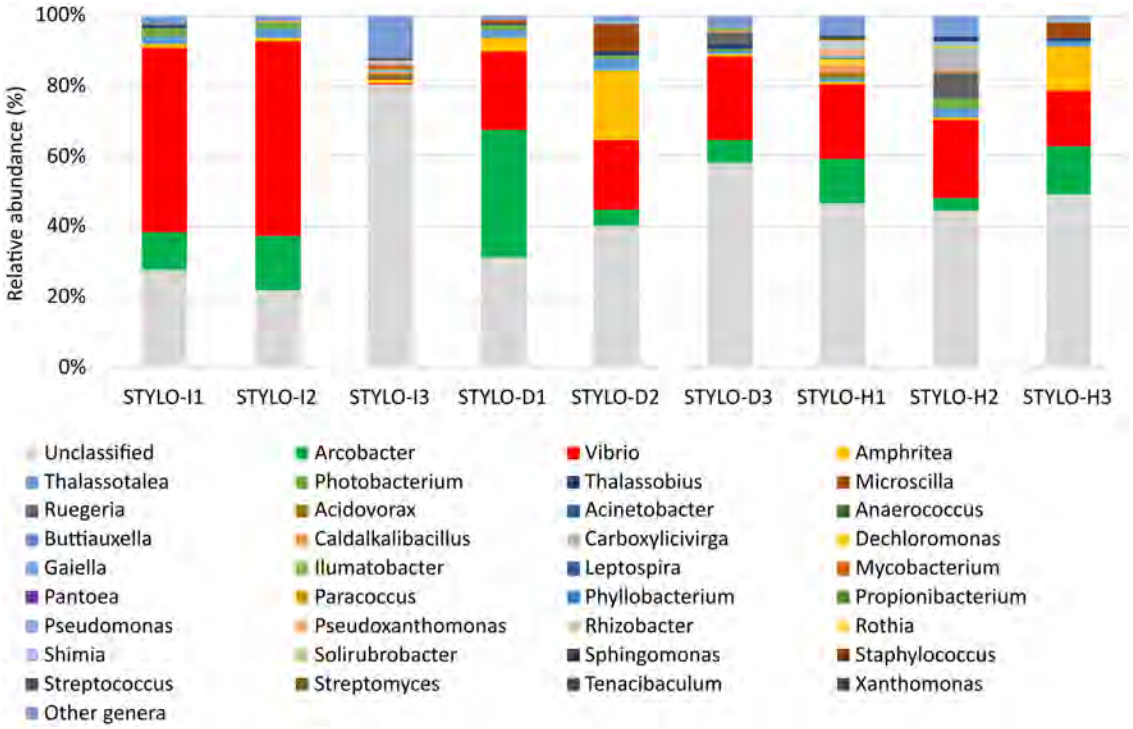

Figure 4. Microbiome analysis

Barplots of the relative abundance of the most abundant genera in each sample; genera with abundance <1% in all samples were grouped in "Other genera." I1, I2, and I3 indicate the intermediate condition; D1, D2, and D3 indicate the "diseased" fragments; H1, H2, and H3 indicate the "healthy" fragments; "STYLO" indicates the coral genus (*Stylophora*).

See also Tables 3, 4, and S4.

Thereafter, a Bonferroni post hoc test was applied. The detailed results of the test are reported in Table S3, while in Figure 3C only the comparison of Teflon vs. films is highlighted for simplicity.

The films loaded with Cipro at all the concentrations tested were capable of completely eradicating the *Vibrio*, confirming the high susceptibility of this bacterium toward this antibiotic, previously noticed in the MIC assay (Teflon vs. films loaded with Cipro: $p < 0.001$). 70P-30C-Gent films at the lowest concentration of 1.0 mg/mL did not show any antibacterial effect, whereas the 50P-50C-Gent showed a mild antibacterial effect ($p < 0.05$). The strongest efficacy was obtained at the highest concentration (5 mg/mL), where 70P-30C-Gent reduced by more than 2 logs the amount of bacteria in the medium (5.5×10^6 CFU, $p < 0.001$), whereas 50P-50C-Gent reduced by about 3 logs the bacteria concentration (1.08×10^6 CFU, $p < 0.001$). This effect could be correlated with the amount of C present in the film composition,[72] which is then covered, but stronger inhibition, probably derived from the higher concentration of antibiotic in the medium (2.5 and 5 mg/mL).

Characterization of the coral disease

Infected colonies of *Stylophora pistillata* were used for the *in vivo* application. Colonies were classified as diseased by the presence of the typical white band on the coral tissue. After the identification of the band, the colonies were visually monitored, and disease progression was used as confirmation of the ongoing infection. Diseased area, color, and velocity of tissue degradation lead us to suspect this disease may present a similar behavior to the RTN disease.[24] Infected fragments were isolated from the mother colonies, which presented a progressing necrosis. Fragments from three diseased colonies were analyzed to study the microbiome and reveal which microorganisms were mainly associated with the infection. A total of 67,257 retained sequences were obtained from the high-throughput sequencing run. The number of sequences retrieved per sample ranged between 507 and 27,474.

The genus *Vibrio* was present in all samples, ranging from 0.28% to 55.27% of the total amount of bacteria (Figure 4; Tables 3, 4, and S4). One-way ANOVA did not show any significant differences ($p = 0.53$) in the percentage of *Vibrio*. Follow-up Bonferroni post hoc test confirmed that no significance was present in the different comparisons among apparently healthy (*Stylophora* [Stylo]-H), intermediate (Stylo-I), and diseased (Stylo-D) tissues (Stylo-D vs. Stylo-H; Stylo-H vs. Stylo-I; and Stylo-I vs. Stylo-D) (Table 4). However, the trend of *Vibrio* percentage over the total amount of bacteria in most of the samples showed an increase in the *Vibrio* genus in the intermediate samples, defined as the area including part of the tissue immediately above and below the threshold of the white band. The amount of *Vibrio* genus in the so-called "diseased" area, defined as the bleached tissue, was comparable to the amount present in the apparently healthy tissue. Thus, the highest concentration of the *Vibrio* genus was found at the threshold of the white band area, although no statistical difference was observed. Further investigation of the *Vibrio* species highlighted the

Table 3. Percentage of sequences classified as *Vibrio* in each sample

	I1	I2	I3	D1	D2	D3	H1	H2	H3
Vibrio	52.30	55.27	0.28	22.30	19.87	23.75	21.26	22.14	15.58

See also Tables 4 and S4; Figure 4.

predominant presence of *V. harveyi* in the analyzed samples (Table S4). The microbiome analysis further confirmed the similarity to the RTN disease, permitting us to classify the treated disease as a tissue-necrosis-like disease.[24,33]

Treatment strategy on infected corals

Four different experimental groups were investigated on the infected fragments: untreated (control), treated with only sealant (BW4LO1), treated with sealant and the film loaded with Cipro (BW4LO1 + Cipro), and treated with sealant and the film loaded with Gent (BW4LO1 + Gent) (Figure 5A). Films with P/C 70:30 were selected for these experiments due to their slightly higher flexibility, crucial for their proper application in hyperbranched corals like *S. pistillata*. To observe the efficacy of the strategy in a real case study, the progression/regression of the disease over 18 weeks was monitored by evaluating whether the fragment was alive and showing signs of unstopped infection, bleaching, necrosis, or other issues that could give any macroscopic feedback comparing them to the control (untreated) infected fragments. Their final status is summarized in Figure 5B. In the control (untreated), the disease advanced rapidly, and already after 6 weeks two of five fragments were dead. Of the remaining control fragments, in two the disease was unstopped, and only one managed to stop the disease and restarted growing by the end of the monitored period. In the group treated with BW4LO1-DIC, the disease initially appeared to slow down in its progression, which may be due to the physical barrier created by the paste; however, after 6 weeks, the disease continued its progression along the coral fragment. At the end of the 18 weeks, the results were similar to those of the control samples: four still infected and one healthy fragment. In the samples treated with BW4LO1-DIC and 70P-30C-Cipro, all the fragments overcame the disease, maintaining their healthy state. Finally, in the samples treated with the 70P-30C-Gent and BW4LO1-DIC films, four fragments were recognized as healthy, and one was still infected.

Statistical analysis using the chi-squared test showed an overall significance of $p < 0.05$ ($\chi^2(3, n = 20) = 10.30$, $p = 0.016$). In particular, this statistical test demonstrated that there is statistical significance in the number of reinfected/dead and non-infected (used as categorical conditions) samples among the treatment groups ($\phi = 0.72$). Finally, considering all the two-component systems used for delivering antibiotics (summing Cipro and Gent treatments), the rate of their success was 90%, significantly higher compared to the 20% of the treatments without antibiotics (untreated control and only the sealant BW4LO1-DIC) which is the natural capacity of the coral to overcome the infection.

Finally, after 8 months of the treatment, new tissue growth was observed in the surviving fragments, both apically (new branches) and basally (base enlargement), by macroscopically observing the sample pictures, and the size of the fragments was compared to that on day 0 (see Figure 5C). In the fragment where the sealant was applied and the lesion stopped (one fragment from BW4LO1-DIC, five fragments from 70P-30C-Cipro + BW4LO1-DIC, and four fragments from 70P-30C-Gent + BW4LO1-DIC), basal growth was observed. Basal tissue growth on the sealant on the fragments treated with Cipro and Gent had already started after 3 months (Figure 5A), while the surviving fragment treated with only the sealant was the slowest in showing signs of basal growth tissue after 4 months on the substrate.

Table 4. Percentage of sequences classified as *Vibrio*, average, and standard deviation for each sample group

Healthy	Intermediate	Diseased
19.66% ± 3.56%	35.95% ± 30.93%	21.97% ± 1.96%

See also Tables 3 and S4; Figure 4.

DISCUSSION

Coral diseases are an emerging multifactorial issue often connected with the increase in chronic environmental stresses, such as pollution or ocean warming and acidification, which are threatening the reef ecosystems.[10,73] Widespread outbreaks have been occurring more often and with more devastating effects.[74] A dramatic example is SCTLD, which has grown to the scale of a marine pandemic in the Caribbean over the last 10 years.[22] Treatments have been developed to manage and slow its progression, with limited success.[25,31,32,75] The absence of treatment strategies for diseased corals should also be addressed in more controlled environments, where small fragments are taken from larger colonies, grown *in situ* or *ex situ*, and transplanted as the final step of coral restoration efforts.[49,76,77] The spread of diseases in coral nurseries and other aquaculture contexts could have critical impacts on restoration efforts, urging for innovative solutions to address coral diseases in various settings.[78–80]

Currently, antibiotics are considered one of the more consolidated options to treat coral diseases induced by bacteria.[31,33,81] Nevertheless, the use of antibiotics often leads to concerns related to the development of antibiotic resistance or the alteration of the microbiome community composition.[82] However, controlled applications, like those presented here, could reduce the risks of antibiotic resistance.[83] These concepts are well established in the field of pharmaceutics and biomedicine, where the use of engineered drug vehicles that reach the target area without releasing their load into the surroundings have managed to reduce the overall dose of the drugs that has a significant effect (effective dose), reducing, at the same time, the collateral effects and eventual phenomena of resistance.[84,85] Similar principles of controlled drug delivery and precise medicine can be applied to cases of coral disease.

Please cite this article in press as: Scribano et al., Eco-friendly active film and sealant for underwater drug delivery to diseased corals, One Earth (2025), https://doi.org/10.1016/j.oneear.2025.101356

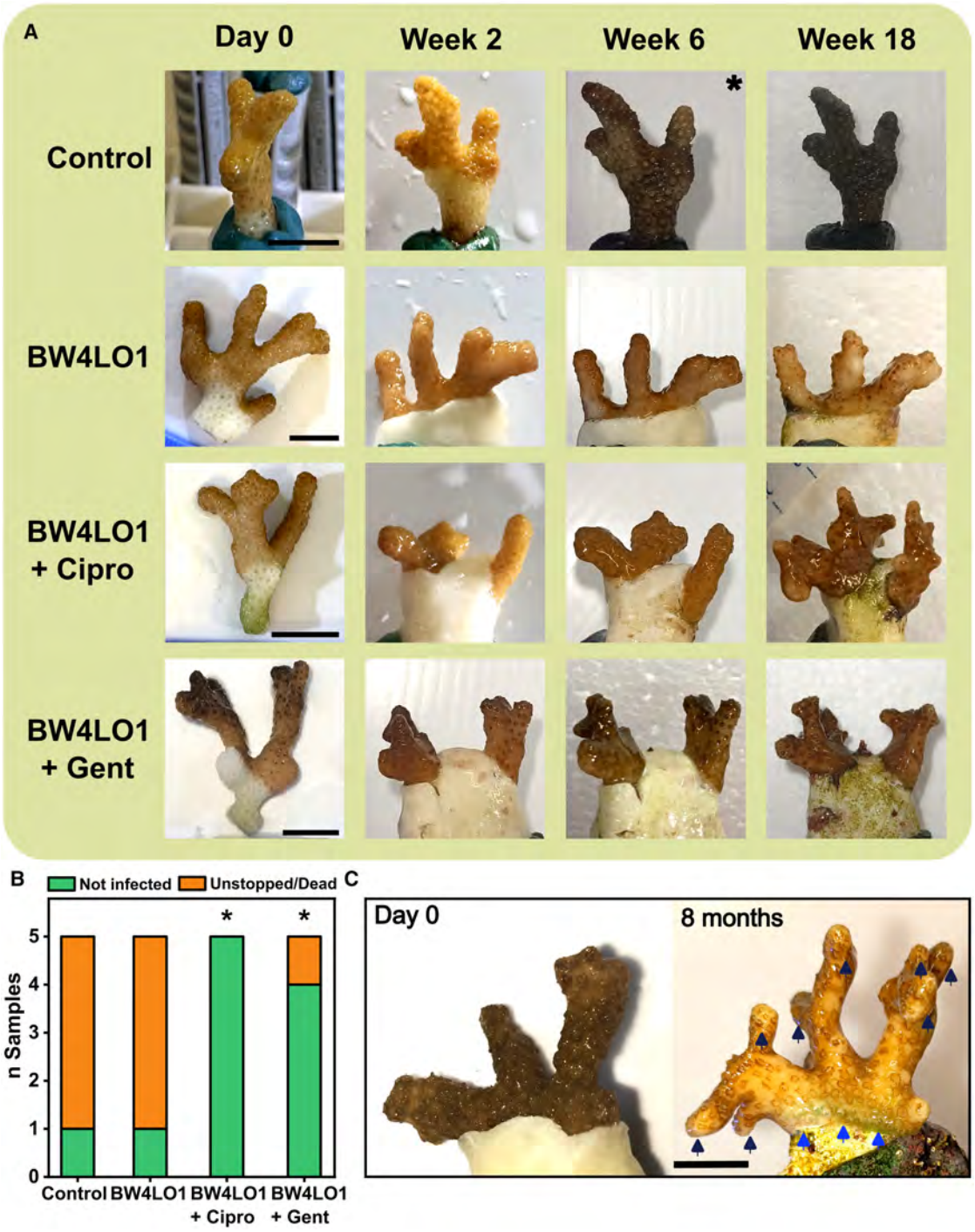

Figure 5. Application of the two-component system in diseased corals

(A) Photographs of infected coral fragments untreated (control), treated with the BW4LO1-DIC, treated with the BW4LO1-DIC + 70P-30C-Cipro, and treated with the BW4LO1-DIC + 70P-30C-Gent over 18 weeks; Asterisk (*) indicates time point at which the fragment died. Scale bar, 1 cm.

(B) Summary of the status of the fragments after 4 months. *$p < 0.05$ ($\chi^2(3, n = 20) = 10.30$, $p = 0.016$).

(C) Apical and basal growth of a single fragment treated with 70P-30C Cipro + BW4LO1-DIC after 8 months; dark-blue arrows indicate apical growth, and light-blue arrows indicate basal growth. Scale bar, 1 cm.

Please cite this article in press as: Scribano et al., Eco-friendly active film and sealant for underwater drug delivery to diseased corals, One Earth (2025), https://doi.org/10.1016/j.oneear.2025.101356

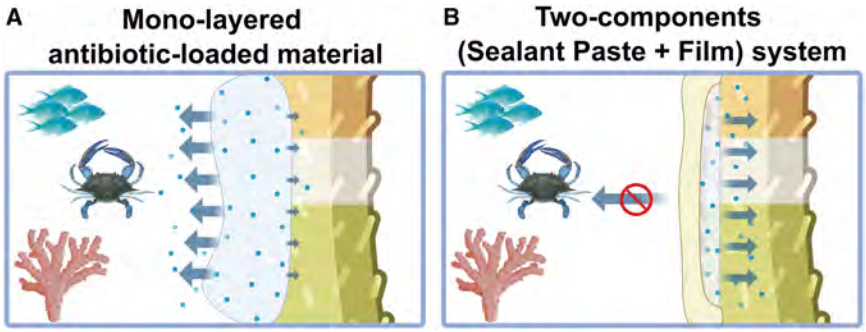

Figure 6. Schematic representation of the sea environment/material/coral infected site interface

The application and drug diffusion of a currently used monolayered antibiotic-loaded material (A) and the two-component antibiotic-loaded system described in this work (B). The size and direction of the arrows indicate the release intensity of the drug (small blue dots) from the materials based on the osmotic pressure given by the water.

Silicon-based ointments and chlorinated epoxy resin matrices are currently used as a free-standing monolayered material.[25,31,32,75,86,87] When they are applied underwater, these treatments can diffuse in two directions: toward coral tissue and the seawater. The diffusion and extraction of the drug from whatever monolayered formulation is strongly mediated by the water through Fick's law, the partition coefficient of the drug, swelling and erosion mechanisms, the hydrophilic or hydrophobic behavior of the matrix, and the concentration and distribution of the drug inside the formulation.[88–90] Therefore, the side exposed to the environment comes into contact with an infinite amount of seawater that undergoes a constant turnover of the solvent, provoking a higher degree of erosion than the internal one. On the other hand, the material side attached to the coral tissue presents a much lower amount of water than the external environment. This principle will drive a difference in the release kinetics and diffusion of the drug between the two interfaces, or so-called compartments, as typically named in the pharmaceutical field. Thus, the drug is expected to constantly and intensively diffuse outside the matrix toward the sea, whereas the diffusion toward the infected area is expected to be significantly less intense (Figure 6A).[48] However, in the infected area where bacteria are proliferating, a constant antibiotic concentration above the MIC should be maintained over time to eradicate the infection.[91]

To improve the antibiotic-based treatments, a two-component system that allows the treatment of the coral-infected sites without the spread of antibiotics in the surrounding water system was proposed in our work (Figure 6B).[92] The system consists of a BW/plant-based sealant and a hydrophilic film composed of P, C, and antibiotics. For the development of the active films, two wide-spectrum antibiotics, Gent and Cipro, were selected, and the MIC was calculated against one of the most concerning coral bacterial pathogens, *V. coralliilyticus*,[44,93] with both showing effectiveness at minimal concentrations of 32.0 and 0.5 μg/mL, respectively. It is worth mentioning that in a previous study, Cipro did not demonstrate the same effectiveness against the same bacterial strain.[44] Nevertheless, in the reported study it is not specified how Cipro was solubilized in water, and, since it is practically insoluble in water, this might have affected the efficacy of the drug. The use of acetic acid to favor the solubilization of Cipro, a strategy applied in our paper, makes it more available to exploit its antibacterial action.[62] Films with different ratios of P and C, polyglycerol as a plasticizer, and loaded with antibiotics at a proportion of 100:1 polymer + plasticizer/drug (w/w) were investigated. Noteworthy is that the quantity of the antibiotics used is much lower compared to previously proposed amoxicillin-loaded silicon paste, with a weight ratio of matrix/antibiotic up to 8:1 (w/w), which has been used as a treatment to stop SCTLD disease progression.[25,32] All the films were transparent and homogeneous, and the two drugs were well dispersed in the polymeric matrices. The films were ductile and stretchable, making them suitable for application on an irregular surface such as corals.

The sealants were prepared using a simple method of melt mixing the BW and the two plant-based oils, followed by quick solidification. The sealant BW4LO1-DIC was chosen as the best candidate, since the development procedure promoted a reorganization of its final semi-crystalline structure that led to a thermo-responsive behavior of its mechanical properties. Commonly, corals live at a temperature between 25°C and 28°C; thus, in this range of temperature, the sealant needs to be solid. At the same time, during the underwater application, the sealant should be malleable and shaped by the operator/diver. As demonstrated by DMTA analysis and measuring the sealant temperature after mixing, BW4LO1-DIC showed a transition phase from a more rigid structure to a moldable material by simply rubbing it with the hands, both in the air and underwater. This feature represents a great technological advancement if compared to the previous work of our group, where a polycaprolactone-*p*-coumaric acid thermoplastic copolymer was utilized as a sealant. Indeed, in this case, to melt and apply the co-polymer, a temperature of 45°C–50°C was necessary, limiting its application at a laboratory or aquarium level.[48]

The unidirectional drug diffusion of the two-component system was confirmed by using a transwell to mimic the sea environment and the coral-infected site, separated by the developed system. Using this approach, we demonstrated (1) the possibility of exclusively and precisely diffusing the antibiotics toward the correct direction of the coral's infected site, making them fully available to exploit their action against the coral bacteria; (2) a safe and eco-friendly use of the antibiotics without releasing them into the sea; and (3) the possibility to apply this strategy directly underwater, as the drug is not immediately diffusing outside of the system, giving time to the operator/diver to apply the two-component system directly underwater. These features enable a new, precise, *in situ* therapy, akin to a first-aid coral kit, suitable for use in both aquaria and the more challenging, yet critical, ocean environments.

Please cite this article in press as: Scribano et al., Eco-friendly active film and sealant for underwater drug delivery to diseased corals, One Earth (2025), https://doi.org/10.1016/j.oneear.2025.101356

As proof of concept, we demonstrated that the proposed system could eradicate the growth of a high concentration of *V. coralliilyticus* (Figure 3C). The two-component system was also applied to corals with a tissue-necrosis-like disease, possibly caused by a *V. harveyi* strain, or at least co-occurring with high abundances of this bacterium, as a result of the microbiome analysis of the lesion. The selected system for this test was composed of BW4LO1-DIC sealant, combined with 70P-30C-Cipro or 70P-30C-Gent, as films with this P/C ratio were more ductile and showed a slightly slower release in the first hours, allowing a suitable application on branched corals. The infected fragments of coral *S. pistillata* were monitored for 18 weeks, and the two-component system for delivering Cipro and Gent stopped the propagation of the infection. The overall yield of lesion halting from the disease reached 90% success, much higher compared to the 20% capacity of the corals in responding to the infection by themselves. Interestingly, after lesion halting, the corals started growing both apically and basally. The basal growth of the material is fundamental because, eventually, the two-component system will be entrapped and included in the structure of the coral. As proved by the BOD test, all the components were fully biodegradable. Note that the BOD test (30 days) is an extreme condition in which biodegradation is exponentially sped up and is not representative of what occurs in a real environment in terms of timescale. Our group has previously tested the degradation of different biocomposite materials in the Maldivian Sea, where the materials started degrading, but the degradation effects were observed on a much larger timescale (months/year compared to days/months in laboratory conditions).[49,56] Similarly, the sealant after 18 weeks looked macroscopically stable, meaning that the biodegradation was occurring slower than the growth rate of the coral tissue to cover it. This is a further innovation that confirms how the proposed technology can be an excellent strategy for treating coral diseases.

The potential short-term antifouling properties of this hydrophobic natural material are noteworthy, as biofouling only started on the sealant after 6 weeks. This feature could be compared to superhydrophobic materials defined as antifouling, such as polydimethylsiloxane (PDMS), on which the fouling appears between 2 and 8 weeks in the underwater environment.[94]

The natural origin of our materials can support an eco-friendly approach to treat coral infections. However, more tests are needed to test for potential impacts on fish and other marine organisms.

To conclude, a new and easy-to-use two-component system for the treatment of coral diseases was successfully developed. The first component was a natural, thermoresponsive, and biodegradable sealant based on BW and plant-based oils to be used and applied underwater on infected corals. The sealant was developed to cover and seal the other component placed onto the infected site of the corals. The second component, based on P, C, and polyglycerol for the delivery of antibiotics Cipro and Gent, was in the form of transparent and stretchable films, developed to be applied in contact with the corals' infected site for their therapy. Its properties were ideal for easy adaptation to the shape of the different corals, expanding its range of application to various species.

When the two-component system was applied to infected corals, it not only led to a yield of successful lesion halting of 90% using one-tenth of the antibiotic amount used previously to treat similar diseases but also allowed the coral regrowth onto the applied materials. This versatile system can be applied in aquaria, where high-density farming of coral fragments occurs, as well as in more challenging environments like coral nurseries or coral reefs in the open sea. Finally, this work highlights once again how merging different scientific disciplines, in this case, pharmaceutics, materials science, and marine ecology, can produce new effective technologies that can help save vital ecosystems such as coral reefs.

METHODS

Materials

Linseed oil (LO) (CAS-No. 8001-26-1), beeswax (BW) (CAS-No. 8012-89-3), chitosan (C) (CAS-No. 9012-76-4), polyvinylpyrrolidone (360 kDa) (P) (CAS-No. 9003-39-8), acetic acid (CAS-No. 64-19-7), ciprofloxacin (Cipro) (CAS-No. 85721-33-1), and gentamicin sulfate (Gent) (CAS-No. 1405-41-0) were purchased from Sigma-Aldrich and used as received. Marine broth 2216 (product no. 76448-500g) was purchased from Millipore and used as suggested by the company. Deionized water was obtained from a Milli-Q Advantage A10 ultrapure water-purification system (Merck-Millipore, Darmstadt, Germany). Polyglycerol-10 was kindly donated by SPIGA NORD (batch no. PG10_2022 1021_0945). Sunflower oil (SFO) was purchased as a commercial product (Olio di semi di girasole Coop) (lot. no. L309323).[95] Sylgard-184 kit (product no. 761028) was purchased from Dow Corning (Midland, MI, USA). *V. coralliilyticus* (strain ATCC BAA-450) was purchased from DSMZ (Braunschweig, Germany).

Preparation of sealant

BW and two natural oils, LO and SFO, with different amounts of C=C in their fatty acid composition, were selected to prepare the sealant. The sealant samples made with BW and the oils SFO and LO, in the weight ratio 4:1, were named BW4SFO1 and BW4LO1, respectively. The components were mixed in an aluminum cup and melted in the oven at 90°C for 5 min. The melted solution was cooled, poured into a glass beaker positioned in a dry ice bath, and stirred until room temperature was reached. These samples were nominated as dry ice cooled, i.e., DIC. Meanwhile, samples cooled without the dry ice bath were called "not DIC" and cooled at room temperature.

Preparation of films

P and C were mixed in a vial, in weight proportions 1:1 (1,050:1,050 mg, called 50P-50C) or 7:3 (1,470:630 mg, called 70P-30C), alongside 20 mL of 8% (v/v) acetic acid aqueous solution and vortexed until fully dispersed. A second aqueous solution of 8% (v/v) acetic acid was also used to solubilize gentamicin or ciprofloxacin at concentrations of 10 mg/mL. In a third acetic acid solution at 8% v/v, polyglycerol-10 at a concentration of 50 mg/mL was dissolved. Subsequently, the polyglycerol-10 solution (8.4 mL) and the antibiotic solution, either with Cipro or Gent (2.542 mL), were added to the solution of P and C. Films without drug were prepared, adding the same amount of acetic acid aqueous solution 8% (v/v) (called "no drug"). The final volume of this solution was brought to 35 mL by adding the aqueous

Please cite this article in press as: Scribano et al., Eco-friendly active film and sealant for underwater drug delivery to diseased corals, One Earth (2025), https://doi.org/10.1016/j.oneear.2025.101356

solution (8% [v/v] acetic acid). The solution was homogenized using a vortex and left stirring for 2 h at 55°C. Finally, the solution was cast on a square Petri dish (120 × 120 mm^2), previously covered with a silicone layer of Sylgard-184, and left to dry in an aspirated hood with a constant flow rate of 0.5 L/min at ambient conditions (16°C–20°C, relative humidity 40%–50%) for 48 h. The final dry weight of each film was approximately 2.55 g. For 50P-50C, the final composition was 41.25% (w/w) of P, 41.25% (w/w) of C, 16.50% (w/w) of polyglycerol-10, and 1% (w/w) of the drug (either Cipro or Gent) films. Likewise, the composition for the 70P-30C was 57.75% (w/w) of P, 24.75% (w/w) of C, 16.50% (w/w) of polyglycerol-10, and 1% (w/w) of drug.

Scanning electron microscopy

The morphology of the films and the sealants was analyzed by SEM using a variable-pressure JOEL JSM-649LA (JEOL, Tokyo, Japan) microscope equipped with a tungsten thermionic electron source and working in high vacuum mode, with an acceleration voltage of 5 kV. The specimens were coated with a 10-nm-thick film of gold utilizing a Cressington 208 HR sputter coater (Cressington, Watford, UK).

Fourier transform infrared spectroscopy

Infrared spectra of all the pastes and films were acquired using an ATR accessory (MIRacle ATR, Pike Technologies) with a diamond crystal coupled to an FTIR spectrometer (Vertex 70v FTIR, Bruker). All spectra were recorded between 4,000 and 600 cm^{-1}, with a resolution of 4 cm^{-1}, accumulating 64 scans.

Thermal analysis

The thermal degradation behavior of the different sealants, including their reagents, was determined by TGA using a TGA Q500 (TA Instruments, USA) instrument. Measurements were carried out using 7–12 mg of sample in a platinum pan under inert N_2 flow (50 mL min^{-1}) in a temperature range from 30°C to 800°C and with a heating rate of 10°C min^{-1}. The weight loss and its first derivative were acquired simultaneously as a function of time/temperature. Curves were normalized at the weight of the sample at 30°C.

Differential scanning calorimetry

Sealant samples were tested with a weight of about 5 mg. An equilibrating phase at 20°C occurred before starting the experiment. The analysis followed the subsequent phases: a rapid cooling at −20°C, an isothermal phase for 1 min, a first melting phase up to 100°C, 1-min isothermal, cooling down to −20°C, 1-min isothermal, and a second melting up to 100°C. Temperature variation was set at 10°C min^{-1}. The machine used was a Discovery DSC 250 with a Discovery RCS90 cooling system and a sample holder from TZero Pans and Lids (aluminum, not sealed).

Deconvolution of the curves was obtained with the software Origin 2022 version 9.9.0.225. The plugin used is "Peak analyzer," and the analysis was performed based on the residuals' first derivative. The summary of the deconvolved curves presented an $R^2 \geq 0.99$.

Dynamic mechanical thermal analysis

DMTA was performed using a DMTA TA Q800 instrument equipped with a compression clamp in frequency sweep mode. Samples of BW4SFO1-DIC, BW4SFO1-not DIC, BW4LO1-DIC, and BW4LO1-not DIC were tested at increasing temperatures, with a rate of 1°C/min, at an interval between 15°C and 50°C ($n = 3$). Experiments were performed in a single-frequency oscillation mode with a frequency of 10 Hz and a displacement amplitude of 5 μm, after a preload of 1 N. Data were recorded every 3 s, and the storage modulus, loss modulus, and tan(δ) as a function of the temperature were evaluated.

Tensile test

The mechanical properties of the films were determined by uniaxial tension tests on a dual-column universal testing machine (Instron 3365). Films were cut in dog-bone shape with a width of 4 mm and an effective length of 25 mm. Displacement was applied at the rate of 20 mm/min. Young's modulus, tensile stress at maximum load, and elongation at break were software-extracted from the resulting curves. Measurements were performed on a minimum of seven pieces per film. All the stress-strain curves were recorded at 25°C and 44% relative humidity.

Water contact angle

The WCA of the sealants was measured using a contact angle goniometer OCA-20 (DataPhysics Instruments, Filderstadt, Germany) at ambient conditions (16°C–20°C, relative humidity 40%–50%). Seawater droplets (5 μL) were laid on the surface, and the contact angle was extracted and calculated from the side view with the help of the software. To ensure repeatability, a minimum of 14 measurements per sample were collected. The DWCA of the films was measured by using the same parameters described above. However, the contact angle was extracted every 1 s for 5 min. To ensure repeatability, three different measurements were taken for each sample.

Sealant temperature variation test

The sealant variation temperature was also tested using a thermometer with a thermocouple (Greisinger GMH 3250) to measure the internal temperature of the paste after hand mixing in the air at room temperature (20°C) and in seawater at 20°C and 25°C. The temperature was measured after poking a hole with a needle in the ball-shaped paste until a constant temperature was reached. When mixed in seawater, the sealant was dried before testing.

Unidirectional drug-release test

A unidirectional drug-release test was constructed and performed to verify that when the two-component system is applied to the corals, the antibiotic will diffuse only in the direction of the infected area and not into the environment. Transwells were used to mimic this condition, and the materials were placed as described in Figure S3D. The transwell structures (VWR tissue culture plate inserts), having a diameter of 6.5 mm and a PET membrane with a porosity of 0.4 μm, were filled first with 6.0-mm film disks, then with 7.0-mm sealant disks, and at the end with 0.25 mL of seawater. Thereafter, the transwell was placed inside another well filled with 1.00 mL of seawater to generate

Please cite this article in press as: Scribano et al., Eco-friendly active film and sealant for underwater drug delivery to diseased corals, One Earth (2025), https://doi.org/10.1016/j.oneear.2025.101356

two different compartments. Seawater was collected from "Old Harbor" di Genoa, Italy, and filtered up to 1.2 μm. The bottom compartment simulated the infected area that should receive the drug, while the upper one inside the transwell mimicked the marine environment. The release experiments were conducted at 25°C, placing the multiwell plate in the incubator to simulate the temperature of the coral reef environment.

Cipro was chosen as a drug model because it has a well-defined absorption spectrum in the UV-visible range, thus allowing us to follow its diffusion from the film into the seawater medium using a CARY 300 Scan UV-visible spectrophotometer. Samples were collected at 15, 30, and 45 min and 1, 2, 3, 4, 6, 24, 30, 48, 54, 72, 78, 144, and 168 h for both compartments. The total volume of seawater in each compartment (upper part 0.25 mL, lower part 1.00 mL) was separately collected at each time point and diluted to a total volume of 2.5 mL, and absorbance was measured using a quartz cuvette in the interval between 600 and 200 nm. The absorption peak at 330 nm was used to monitor the diffusion of Cipro. The test was repeated in triplicate, and the results are expressed as mean and standard deviation.

Biochemical oxygen demand

BOD was used to investigate the biodegradability of the samples. The test followed ISO 23977-2: 2020, which standardizes how to measure the biochemical oxygen demand in seawater over 30 days. Samples of films and sealants were cut into small pieces, and about 50 mg of material was added to 432 mL of seawater collected at the "Old Harbor" of Genoa, Italy. The experiment was performed using OxiTop-IDS measuring heads following the protocol suggested by the manufacturer. Biotic consumption of the oxygen present in the free volume of the system was measured as a function of the decrease in pressure. Raw oxygen consumption data (mg O_2/L) were corrected by subtracting the mean values of the blanks obtained by measuring the seawater's oxygen consumption without any test material. After this subtraction, values were normalized on the mass of the individual samples and referred to as milligrams of oxygen consumed per 100 mg of material in 1 L of seawater (mg O_2/100 mg).

Minimal inhibitory concentration

MIC assay was performed in a 12-well multiwell, using 2 mL per well of sterilized marine broth medium inoculated with *V. coralliilyticus* at a concentration of 1.7×10^9 CFU, corresponding to OD_{600nm} 0.01. In each well, the drug concentration was doubled, from 0.125 up to 64 μg/mL. The tested drugs were Cipro and Gent. The MIC was evaluated after 24 h of incubation under constant shaking (100 rpm) at 28°C through the measurement of optical density at 600 nm using a UV-visible spectrophotometer. Initial solutions were prepared as follows: 10 mg of Gent was dissolved in 1 mL of Milli-Q water, whereas 10 mg of Cipro was dissolved in 980 μL of Milli-Q water and 20 μL of acetic acid. Serial dilution was followed as described above. The results were classified as R (resistant), I (intermediate), and S (susceptible), based on the efficacy of the drug dose administered.[96]

Disk-diffusion assay

The disk-diffusion assay was performed on sterilized marine agar Petri dishes. In each Petri dish, 200 μL of *V. coralliilyticus* at 3.4×10^{10} CFU (OD_{600nm} 0.2) were plated, and three 6.0-mm disks were positioned on top after drying. Inhibitory growth diameter was measured after 24 h. Controls were prepared using 6.0-mm sterilized filter paper with 5 μL of either growth medium (negative control) or 5 mg/mL apramycin (positive control). Maximum diameters were measured using the line function of ImageJ using the Petri dish dimension as a scale bar (90 mm). The maximum diameter statistic was derived using a one-way ANOVA followed by a Bonferroni post hoc test, with a significance level set at $\alpha = 0.05$. Groups that do not share a common letter are significantly different (Figure 3B).

Growth analysis in liquid

Growth analysis was also performed in a solution of marine broth with an optical density of *V. coralliilyticus* of 1.7×10^6 CFU (OD_{600nm} 0.01). Three antibiotic concentrations were tested: 5.0, 2.5, and 1.0 mg/mL of film in triplicate. The film pieces were previously sterilized with UV light, 10 min/side. Subsequently, the films were covered with the previously mentioned medium (2 mL) and incubated at 28°C for 24 h with 100 rpm of shaking. The concentration was initially measured by optical density at the T_0 of the experiment (OD_{600nm} 0.01, ~10^6 CFU). After 24 h, an aliquot (10 μL) of each triplicate was plated to count the surviving CFU, and the concentration after growth was derived. The statistic was calculated on the concentration after 24 h of growth using a two-way ANOVA followed by a Bonferroni post hoc test with a significance level of $\alpha = 0.05$. An inert Teflon film was used as a positive control. A blank was also prepared to test bacterial growth in the medium (no antibiotics or materials) after initial inoculation (OD = 0.01 at T_0). The blank was not included in the statistical test as it did not present any comparable film concentration.

Maintenance and growth conditions of corals

The reef-building coral *Stylophora pistillata*, a standard coral species model farmed and reproduced at the Genoa Aquarium, was used for this experiment. Fragments from three infected colonies of *S. pistillata* were fed twice a week with a food mixture in a solution containing *Tetraselmis* sp. algae and Rotifera.

During the day, the tank was set up as a semi-open system, and the temperature was set at 25°C (by exchange heater). The water was pumped from a depth of 50 m outside the harbor of Genoa, then filtered (with a sand filter) and sterilized (by UV filtration), and finally supplied with a flow rate of 0.3 $m^3\ h^{-1}$.

During the night, the tank was set up as a closed system, hence the seawater from the tank passed through a filtration system comprising a sand filter (0.4 mm, Astralpool ARTIC) and a UV light (Panaque 750 s, with four 40-W lamps embedded), and subsequently reinserted in the tank. The water circulation pump (Argonaut av150-2dn-sb 220v) was set to 10–13 $m^3\ h^{-1}$ to ensure total water filtration every 25 min.

Corals were illuminated with an HQI lamp (400-W 10,000 K Nepturion BLV, 12:12 h light/dark) at an average irradiance of 250 μmol photons $m^{-2}\ s^{-1}$. Moreover, 50 L of calcium hydroxide solution at a concentration of 18 g/L was added dropwise every night to facilitate the calcification of corals, enhancing their growth. Subsequently, 20 *S. pistillata* fragments were isolated to prevent other colonies' infections at 25°C in another 400-L tank (13:11 h light/dark) illuminated with an LED light (62 W,

5,000 K) at an average irradiance of 200 μmol photons m^{-2} s^{-1} and a complete water change every hour. The water filtration and heating systems are the same as reported in Contardi et al.[50]

Characterization of tissue-necrosis-like disease

S. pistillata fragments were classified as ''apparently healthy,'' ''intermediate,'' and ''diseased.'' In particular, the samples analyzed were fragmented from specific coral areas. The apparently healthy tissue was part of the fragment where the tissue did not show any macroscopic signs of disease or bleaching, placed at least 1.5 cm above the visible threshold of the white band; the intermediate samples were collected, including part of the tissue immediately above and below the white band threshold; finally, the fully white tissue directly above the necrotic tissue was considered as the diseased portion.

For DNA extraction, total DNA was extracted from nine ground coral fragments (three for each group) of approximately 1 cm × 2 cm, using a FastDNA Spin kit for Soil (MP Biomedicals, Solon, OH, USA) according to manufacturer's instructions. Extracted DNA was further purified with a Monarch Genomic DNA Purification Kit (New England BioLabs, Ipswich, MA, USA) to avoid nucleic acid degradation over time.

For PCR amplification, a fragment containing the V5-V6 hypervariable regions of the bacterial 16S rRNA gene was PCR amplified with barcoded primers to allow sample pooling and sequence sorting, as previously described.[97]

For high-throughput sequencing, amplicons were sequenced by MiSeq Illumina (Illumina, San Diego, CA, USA) with a 2 × 300-bp paired-end protocol. Amplicon sequence variants (ASVs) were inferred using the DADA2 pipeline,[98] as previously described.[99] ASVs shorter than the expected size were checked by BLAST (Basic Local Alignment Search Tool) and discarded if they did not match any bacterial strains. ASVs taxonomically classified as non-bacterial (archaea; not assigned domain) were also discarded. Finally, ASVs that were classified as belonging to genus *Vibrio* were also tentatively assigned to one or more species by BLAST, selecting, for each ASV, up to four ''best hit'' species according to the lowest E value.

The proportion of bacteria that were *Vibrio* in each sample group was compared using a one-way ANOVA and post hoc Bonferroni test with a significance level of $\alpha = 0.05$.

Application of the two-component system on infected corals

Twenty fragments were derived from three different diseased mother colonies. For each experimental group, five fragments were randomly assigned. Photographs of diseased fragments untreated (control), treated with only the sealant BW4LO1-DIC, treated with the sealant BW4LO1-DIC + film 70P-30C-Cipro, and treated with the sealant BW4LO1-DIC + film 70P-30C-Gent were acquired every 2 weeks for 4 months to monitor the disease progression.

The hydrophilic films were easily fixed onto the coral branches and applied to the white band of the disease by cutting them into pieces with sterile blades, positioning them, and letting them adhere to the coral surface. The sealant was then warmed by hand mixing and rubbing before being applied on top of the film, covering it completely. To prevent bacterial contamination among the samples, the treatment was applied using sterile gloves for each application. The white band represents the infected area and the disease's progression. To ensure the therapy was applied to all potentially infected areas, the films were placed over the lesion (white band) and extended 1 cm beyond the edges of the lesion.

At the end of the experiment, samples were classified as ''unstopped infection/dead'' or ''not infected'' and analyzed as categorical data. Statistical analysis of categorical data was performed using a chi-squared test analyzing the association between the groups and the condition at the end of the experiment. Significance was set for $p < 0.05$.

RESOURCE AVAILABILITY

Lead contact

Requests for further information and resources should be directed to and will be fulfilled by the lead contact, Marco Contardi (marco.contardi@unimib.it).

Materials availability

This study did not generate new unique reagents.

Data and code availability

Raw data have been deposited at zenodo.org and are publicly available as of the date of publication at Zenodo: https://doi.org/10.5281/zenodo.15560870.

ACKNOWLEDGMENTS

The authors would like to declare that part of this research was funded under the National Recovery and Resilience Plan (NRRP), Mission 4 Component 2 Investment 1.4 – Call for tender no. 3138 of 16 December 2021, rectified by Decree n.3175 of December 18, 2021 of the Italian Ministry of University and Research funded by the European Union – NextGenerationEU. Project code CN_00000033, Concession Decree no. 1034 of June 17, 2022 adopted by the Italian Ministry of University and Research, CUP J33C22001200001, Project title ''National Biodiversity Future Center – NBFC.'' This work is part of the ''Technologies for Sustainability'' flagship program of the Italian Institute of Technology (IIT). The authors thank L. Marini for TGA and DSC measurements and G. Mancini for the sealant temperature variation test.

AUTHOR CONTRIBUTIONS

V.S.: conceptualization, data curation, formal analysis, investigation, visualization, writing – original draft, and writing – review & editing. M.C.: conceptualization, data curation, formal analysis, investigation, visualization, supervision, writing – original draft, and writing – review & editing; C.R.: formal analysis and investigation. V.I.: formal analysis, investigation, and writing – original draft. F. F.: formal analysis and investigation. L.C.: formal analysis and investigation. I. Gandolfi: formal analysis and investigation. I. Ghizzi: formal analysis and investigation. S.L.: investigation and resources. P.G.: resources and writing – review & editing. S.M.: conceptualization, resources, supervision, writing – original draft, and writing – review & editing. A.A.: conceptualization, resources, supervision, funding acquisition, and writing – review & editing. M.C., S.M., and A.A. have been designated as corresponding authors because they have a crucial and leading role in the supervision and management of authors, resources, and funding between the Istituto Italiano di Tecnologia (IIT) and the University of Milano-Bicocca, which are two of many institutions from where the presented technology has been conceptualized, designed, and fabricated.

DECLARATION OF INTERESTS

The authors declare that they have no known competing financial interests or personal relationships that could have appeared to influence the work reported in this paper.

SUPPLEMENTAL INFORMATION

Supplemental information can be found online at https://doi.org/10.1016/j.oneear.2025.101356.

Received: October 16, 2024
Revised: February 24, 2025
Accepted: June 7, 2025

REFERENCES

1. Knowlton, N., and Rohwer, F. (2003). Multispecies Microbial Mutualisms on Coral Reefs: The Host as a Habitat. Am. Nat. *162*, S51–S62. https://doi.org/10.1086/378684.
2. Liu, Y., Wu, H., Shu, Y., Hua, Y., and Fu, P. (2024). Symbiodiniaceae and Ruegeria sp. Co-Cultivation to Enhance Nutrient Exchanges in Coral Holobiont. Microorganisms *12*, 1217. https://doi.org/10.3390/microorganisms12061217.
3. Pollock, F.J., McMinds, R., Smith, S., Bourne, D.G., Willis, B.L., Medina, M., Thurber, R.V., and Zaneveld, J.R. (2018). Coral-associated bacteria demonstrate phylosymbiosis and cophylogeny. Nat. Commun. *9*, 4921. https://doi.org/10.1038/s41467-018-07275-x.
4. Apprill, A., Weber, L.G., and Santoro, A.E. (2016). Distinguishing between Microbial Habitats Unravels Ecological Complexity in Coral Microbiomes. mSystems *1*, e00143-16. https://doi.org/10.1128/mSystems.00143-16.
5. Sweet, M.J., and Bulling, M.T. (2017). On the Importance of the Microbiome and Pathobiome in Coral Health and Disease. Front. Mar. Sci. *4*, 9. https://doi.org/10.3389/fmars.2017.00009.
6. Sheikh, H.I., Najiah, M., Fadhlina, A., Laith, A.A., Nor, M.M., Jalal, K.C.A., and Kasan, N.A. (2022). Temperature Upshift Mostly but not Always Enhances the Growth of Vibrio Species: A Systematic Review. Front. Mar. Sci. *9*. https://doi.org/10.3389/fmars.2022.959830.
7. Fox-Kemper, B., Hewitt, H.T., and Xiao, C. (2021). Ocean, cryosphere and sea level change. In Climate Change 2021 - The Physical Science Basis. Contribution of Working Group I to the Sixth Assessment Report of the Intergovernmental Panel on Climate Change, V. Masson-Delmotte, P. Zhai, A. Pirani, S.L. Connors, C. Péan, S. Berger, N. Caud, Y. Chen, L. Goldfarb, and M.I. Gomis, et al., eds. (Cambridge University Press), pp. 1211–1362.
8. Apprill, A. (2017). Marine Animal Microbiomes: Toward Understanding Host-Microbiome Interactions in a Changing Ocean. Front. Mar. Sci. *4*, 222. https://doi.org/10.3389/fmars.2017.00222.
9. Pinzón, J.H., Kamel, B., Burge, C.A., Harvell, C.D., Medina, M., Weil, E., and Mydlarz, L.D. (2015). Whole transcriptome analysis reveals changes in expression of immune-related genes during and after bleaching in a reef-building coral. Roy Soc Open Sci *2*, 140214. https://doi.org/10.1098/rsos.140214.
10. Burke, S., Pottier, P., Lagisz, M., Macartney, E.L., Ainsworth, T., Drobniak, S.M., and Nakagawa, S. (2023). The impact of rising temperatures on the prevalence of coral diseases and its predictability: A global meta-analysis. Ecol. Lett. *26*, 1466–1481. https://doi.org/10.1111/ele.14266.
11. Rosales, S.M., Miller, M.W., Williams, D.E., Traylor-Knowles, N., Young, B., and Serrano, X.M. (2019). Microbiome differences in disease-resistant vs. susceptible corals subjected to disease challenge assays. Sci. Rep. *9*, 18279. https://doi.org/10.1038/s41598-019-54855-y.
12. Shore, A., and Caldwell, J.M. (2019). Modes of coral disease transmission: how do diseases spread between individuals and among populations? Mar. Biol. *166*, 45. https://doi.org/10.1007/s00227-019-3490-8.
13. Moriarty, T., Leggat, W., Huggett, M.J., and Ainsworth, T.D. (2020). Coral Disease Causes, Consequences, and Risk within Coral Restoration. Trends Microbiol. *28*, 793–807. https://doi.org/10.1016/j.tim.2020.06.002.
14. Strudwick, P., Camp, E.F., Seymour, J., Roper, C., Edmondson, J., Howlett, L., and Suggett, D.J. (2024). Impacts of plastic-free materials on coral-associated bacterial communities during reef restoration. Environ. Microbiol. Rep. *16*, e13229. https://doi.org/10.1111/1758-2229.13229.
15. Beloe, C.J., Browne, M.A., and Johnston, E.L. (2022). Plastic Debris As a Vector for Bacterial Disease: An Interdisciplinary Systematic Review. Environ. Sci. Technol. *56*, 2950–2958. https://doi.org/10.1021/acs.est.1c05405.
16. Sweet, M., and Bythell, J. (2017). The role of viruses in coral health and disease. J. Invertebr. Pathol. *147*, 136–144. https://doi.org/10.1016/j.jip.2016.12.005.
17. Roik, A., Reverter, M., and Pogoreutz, C. (2022). A roadmap to understanding diversity and function of coral reef-associated fungi. FEMS Microbiol. Rev. *46*, fuac028. https://doi.org/10.1093/femsre/fuac028.
18. Gleason, F.H., Gadd, G.M., Pitt, J.I., and Larkum, A.W.D. (2017). The roles of endolithic fungi in bioerosion and disease in marine ecosystems. II. Potential facultatively parasitic anamorphic ascomycetes can cause disease in corals and molluscs. Mycology *8*, 216–227. https://doi.org/10.1080/21501203.2017.1371802.
19. Akmal, K.F., Shahbudin, S., Abdul Muhaimin, Z., Shah, M.D., and Chong, W.S. (2023). Application of Biotechnology in White Syndrome Coral Disease Identification. In Marine Biotechnology: Applications in Food, Drugs and Energy, M.D. Shah, J. Ransangan, and B.A. Venmathi Maran, eds. (Springer Nature Singapore), pp. 271–297. https://doi.org/10.1007/978-981-99-0624-6_13.
20. Miller, A.W., and Richardson, L.L. (2011). A meta-analysis of 16S rRNA gene clone libraries from the polymicrobial black band disease of corals. FEMS Microbiol. Ecol. *75*, 231–241. https://doi.org/10.1111/j.1574-6941.2010.00991.x.
21. Papke, E., Carreiro, A., Dennison, C., Deutsch, J.M., Isma, L.M., Meiling, S.S., Rossin, A.M., Baker, A.C., Brandt, M.E., Garg, N., et al. (2024). Stony coral tissue loss disease: a review of emergence, impacts, etiology, diagnostics, and intervention. Front. Mar. Sci. *10*. https://doi.org/10.3389/fmars.2023.1321271.
22. Precht, W.F., Gintert, B.E., Robbart, M.L., Fura, R., and van Woesik, R. (2016). Unprecedented Disease-Related Coral Mortality in Southeastern Florida. Sci. Rep. *6*, 31374. https://doi.org/10.1038/srep31374.
23. Sheridan, C., Kramarsky-Winter, E., Sweet, M., Kushmaro, A., and Leal, M.C. (2013). Diseases in coral aquaculture: causes, implications and preventions. Aquaculture *396–399*, 124–135. https://doi.org/10.1016/j.aquaculture.2013.02.037.
24. Luna, G.M., Biavasco, F., and Danovaro, R. (2007). Bacteria associated with the rapid tissue necrosis of stony corals. Environ. Microbiol. *9*, 1851–1857. https://doi.org/10.1111/j.1462-2920.2007.01287.x.
25. Neely, K.L., Shea, C.P., Macaulay, K.A., Hower, E.K., and Dobler, M.A. (2021). Short- and Long-Term Effectiveness of Coral Disease Treatments. Front. Mar. Sci. *8*, 675349. https://doi.org/10.3389/fmars.2021.675349.
26. Beurmann, S., Runyon, C.M., Videau, P., Callahan, S.M., and Aeby, G.S. (2017). Assessment of disease lesion removal as a method to control chronic white syndrome. Dis. Aquat. Organ. *123*, 173–179. https://doi.org/10.3354/dao03088.
27. Thatcher, C., Hoj, L., and Bourne, D.G. (2022). Probiotics for coral aquaculture: challenges and considerations. Curr Opin Biotech *73*, 380–386. https://doi.org/10.1016/j.copbio.2021.09.009.
28. Roger, L.M., Lewinski, N.A., Putnam, H.M., Roxbury, D., Tresguerres, M., and Wangpraseurt, D. (2023). Nanobiotech engineering for future coral reefs. One Earth *6*, 778–789. https://doi.org/10.1016/j.oneear.2023.05.008.
29. Atad, I., Zvuloni, A., Loya, Y., and Rosenberg, E. (2012). Phage therapy of the white plague-like disease of Favia favus in the Red Sea. Coral Reefs *31*, 665–670. https://doi.org/10.1007/s00338-012-0900-5.
30. Sweet, M.J., Croquer, A., and Bythell, J.C. (2014). Experimental antibiotic treatment identifies potential pathogens of white band disease in the endangered Caribbean coral Acropora cervicornis. Proc. Biol. Sci. *281*, 20140094. https://doi.org/10.1098/rspb.2014.0094.

31. Shilling, E.N., Combs, I.R., and Voss, J.D. (2021). Assessing the effectiveness of two intervention methods for stony coral tissue loss disease on. Sci. Rep. *11*, 8566. https://doi.org/10.1038/s41598-021-86926-4.

32. Neely, K.L., Macaulay, K.A., Hower, E.K., and Dobler, M.A. (2020). Effectiveness of topical antibiotics in treating corals affected by Stony Coral Tissue Loss Disease. PeerJ *8*, e9289. https://doi.org/10.7717/peerj.9289.

33. Sweet, M., Jones, R., and Bythell, J. (2012). Coral diseases in aquaria and in nature. J. Mar. Biol. Assoc. U. K. *92*, 791–801. https://doi.org/10.1017/S0025315411001688.

34. Toth, K.A., Buckley, S.F., Noren, H., Neely, K.L., and Walker, B.K. (2024). Broadscale coral disease interventions elicit efficiencies in endemic disease response. Front. Mar. Sci. *10*. https://doi.org/10.3389/fmars.2023.1302697.

35. Paul, A., Laurila, T., Vuorinen, V., and Divinski, S.V. (2014). Fick's laws of diffusion. Thermodynamics, Diffusion and the Kirkendall Effect in Solids, 115–139.

36. Saranjampour, P., Vebrosky, E.N., and Armbrust, K.L. (2017). Salinity Impacts on Water Solubility and n-Octanol/Water Partition Coefficients of Selected Pesticides and Oil Constituents. Environ. Toxicol. Chem. *36*, 2274–2280. https://doi.org/10.1002/etc.3784.

37. Lehner, F.K. (1979). On the validity of Fick's law for transient diffusion through a porous medium. Chem. Eng. Sci. *34*, 821–825.

38. Visan, A.I., Popescu-Pelin, G., and Socol, G. (2021). Degradation Behavior of Polymers Used as Coating Materials for Drug Delivery-A Basic Review. Polymers *13*, 1272. https://doi.org/10.3390/polym13081272.

39. Liu, Y., Shi, L., Su, L., van der Mei, H.C., Jutte, P.C., Ren, Y., and Busscher, H.J. (2019). Nanotechnology-based antimicrobials and delivery systems for biofilm-infection control. Chem. Soc. Rev. *48*, 428–446. https://doi.org/10.1039/c7cs00807d.

40. Wu, P., and Grainger, D.W. (2006). Drug/device combinations for local drug therapies and infection prophylaxis. Biomaterials *27*, 2450–2467. https://doi.org/10.1016/j.biomaterials.2005.11.031.

41. Smith, A.W. (2005). Biofilms and antibiotic therapy: Is there a role for combating bacterial resistance by the use of novel drug delivery systems? Adv. Drug Deliv. Rev. *57*, 1539–1550. https://doi.org/10.1016/j.addr.2005.04.007.

42. Connelly, M.T., McRae, C.J., Liu, P.J., Martin, C.E., and Traylor-Knowles, N. (2022). Antibiotics Alter Coral-Symbiodiniaceae Bacteria Interactions and Cause Microbial Dysbiosis During Heat Stress. Front. Mar. Sci. *08*, 814124. https://doi.org/10.3389/fmars.2021.814124.

43. Connelly, M.T., Snyder, G., Palacio-Castro, A.M., Gillette, P.R., Baker, A.C., and Traylor-Knowles, N. (2023). Antibiotics reduce coral-associated bacteria diversity, decrease holobiont oxygen consumption and activate immune gene expression. Mol. Ecol. *32*, 4677–4694. https://doi.org/10.1111/mec.17049.

44. Vizcaino, M.I., Johnson, W.R., Kimes, N.E., Williams, K., Torralba, M., Nelson, K.E., Smith, G.W., Weil, E., Moeller, P.D.R., and Morris, P.J. (2010). Antimicrobial Resistance of the Coral Pathogen Vibrio coralliilyticus and Caribbean Sister Phylotypes Isolated from a Diseased Octocoral. Microb. Ecol. *59*, 646–657. https://doi.org/10.1007/s00248-010-9644-3.

45. MacVittie, S., Doroodian, S., Alberto, A., and Sogin, M. (2024). Microbiome depletion and recovery in the sea anemone, following antibiotic exposure. mSystems *9*, e0134223. https://doi.org/10.1128/msystems.01342-23.

46. Adebisi, Y.A. (2023). Balancing the risks and benefits of antibiotic use in a globalized world: the ethics of antimicrobial resistance. Global. Health *19*, 27. https://doi.org/10.1186/s12992-023-00930-z.

47. Sonawane, M., Shinkar, D., and R.. (2017). Mucoadhesive buccal drug delivery system: review article. Int. J. Curr. Pharm. Res. *9*, 1–4. https://doi.org/10.22159/ijcpr.2017v9i4.20960.

48. Contardi, M., Montano, S., Liguori, G., Heredia-Guerrero, J.A., Galli, P., Athanassiou, A., and Bayer, I.S. (2020). Treatment of Coral Wounds by Combining an Antiseptic Bilayer Film and an Injectable Antioxidant Biopolymer. Sci. Rep. *10*, 988. https://doi.org/10.1038/s41598-020-57980-1.

49. Zych, A., Contardi, M., Rinaldi, C., Scribano, V., Isa, V., Kossyvaki, D., Gobbato, J., Ceseracciu, L., Lavorano, S., Galli, P., et al. (2024). Underwater Quick-Hardening Vegetable Oil-Based Biodegradable Putty for Sustainable Coral Reef Restoration and Rehabilitation. Adv. Sustain. Syst. *8*, 202400110. https://doi.org/10.1002/adsu.202400110.

50. Contardi, M., Fadda, M., Isa, V., Louis, Y.D., Madaschi, A., Vencato, S., Montalbetti, E., Bertolacci, L., Ceseracciu, L., Seveso, D., et al. (2023). Biodegradable Zein-Based Biocomposite Films for Underwater Delivery of Curcumin Reduce Thermal Stress Effects in Corals. ACS Appl. Mater. Interfaces *15*, 33916–33931. https://doi.org/10.1021/acsami.3c01166.

51. Wu, T., Zivanovic, S., Draughon, F.A., Conway, W.S., and Sams, C.E. (2005). Physicochemical Properties and Bioactivity of Fungal Chitin and Chitosan. J. Agric. Food Chem. *53*, 3888–3894. https://doi.org/10.1021/jf048202s.

52. Teodorescu, M., and Bercea, M. (2015). Poly(vinylpyrrolidone) – A Versatile Polymer for Biomedical and Beyond Medical Applications. Polym.-Plast. Technol. Eng. *54*, 923–943. https://doi.org/10.1080/03602559.2014.979506.

53. Contardi, M., Kossyvaki, D., Picone, P., Summa, M., Guo, X., Heredia-Guerrero, J.A., Giacomazza, D., Carzino, R., Goldoni, L., Scoponi, G., et al. (2021). Electrospun polyvinylpyrrolidone (PVP) hydrogels containing hydroxycinnamic acid derivatives as potential wound dressings. Chem. Eng. J. *409*, 128144. https://doi.org/10.1016/j.cej.2020.128144.

54. Inkson, B.J. (2016). 2 - Scanning electron microscopy (SEM) and transmission electron microscopy (TEM) for materials characterization. In Materials Characterization Using Nondestructive Evaluation (NDE) Methods, G. Hübschen, I. Altpeter, R. Tschuncky, and H.-G. Herrmann, eds. (Woodhead Publishing), pp. 17–43. https://doi.org/10.1016/B978-0-08-100040-3.00002-X.

55. Donald, A.M. (2003). The use of environmental scanning electron microscopy for imaging wet and insulating materials. Nat. Mater. *2*, 511–516. https://doi.org/10.1038/nmat898.

56. Contardi, M., Montano, S., Galli, P., Mazzon, G., Mah'd Moh'd Ayyoub, A., Seveso, D., Saliu, F., Maggioni, D., Athanassiou, A., and Bayer, I.S. (2021). Marine Fouling Characteristics of Biocomposites in a Coral Reef Ecosystem. Adv. Sustain. Syst. *5*, 2100089. https://doi.org/10.1002/adsu.202100089.

57. Contardi, M., Heredia-Guerrero, J.A., Guzman-Puyol, S., Summa, M., Benítez, J.J., Goldoni, L., Caputo, G., Cusimano, G., Picone, P., Di Carlo, M., et al. (2019). Combining dietary phenolic antioxidants with polyvinylpyrrolidone: transparent biopolymer films based on p-coumaric acid for controlled release. J. Mater. Chem. B *7*, 1384–1396. https://doi.org/10.1039/c8tb03017k.

58. Pohl, T., Al-Muqdadi, S.W., Ali, M.H., Fawzi, N.A.-M., Ehrlich, H., and Merkel, B. (2014). Discovery of a living coral reef in the coastal waters of Iraq. Sci. Rep. *4*, 4250. https://doi.org/10.1038/srep04250.

59. Howells, E.J., Abrego, D., Meyer, E., Kirk, N.L., and Burt, J.A. (2016). Host adaptation and unexpected symbiont partners enable reef-building corals to tolerate extreme temperatures. Glob. Chang. Biol. *22*, 2702–2714. https://doi.org/10.1111/gcb.13250.

60. Bajzek, T.J. (2005). Thermocouples: A sensor for measuring temperature. IEEE Instrum Meas Mag *8*, 35–40. https://doi.org/10.1109/Mim.2005.1405922.

61. Contardi, M., Russo, D., Suarato, G., Heredia-Guerrero, J.A., Ceseracciu, L., Penna, I., Margaroli, N., Summa, M., Spanò, R., Tassistro, G., et al. (2019). Polyvinylpyrrolidone/hyaluronic acid-based bilayer constructs for sequential delivery of cutaneous antiseptic and antibiotic. Chem. Eng. J. *358*, 912–923. https://doi.org/10.1016/j.cej.2018.10.048.

62. Contardi, M., Heredia-Guerrero, J.A., Perotto, G., Valentini, P., Pompa, P.P., Spanò, R., Goldoni, L., Bertorelli, R., Athanassiou, A., and Bayer, I.S. (2017). Transparent ciprofloxacin-povidone antibiotic films and nanofiber mats as potential skin and wound care dressings. Eur. J. Pharm. Sci. *104*, 133–144. https://doi.org/10.1016/j.ejps.2017.03.044.

63. Contardi, M., Ayyoub, A.M.M., Summa, M., Kossyvaki, D., Fadda, M., Liessi, N., Armirotti, A., Fragouli, D., Bertorelli, R., and Athanassiou, A. (2022). Self-Adhesive and Antioxidant Poly(vinylpyrrolidone)/Alginate-Based Bilayer Films Loaded with Extracts as Potential Skin Dressings. ACS Appl. Bio Mater. *5*, 2880–2893. https://doi.org/10.1021/acsabm.2c00254.

64. Nardi, M., Ceseracciu, L., Scribano, V., Contardi, M., Athanassiou, A., and Zych, A. (2024). Sustainable adhesives: Exploring boronic ester vitrimers containing lignin microparticles. Chem. Eng. J. *495*, 153400. https://doi.org/10.1016/j.cej.2024.153400.

65. Davis, J.R. (2004). Tensile Testing (ASM international).

66. Tagliaro, I., Mariani, M., Akbari, R., Contardi, M., Summa, M., Saliu, F., Nisticò, R., and Antonini, C. (2024). PFAS-free superhydrophobic chitosan coating for fabrics. Carbohyd Polym *333*, 121981. https://doi.org/10.1016/j.carbpol.2024.121981.

67. Murgia, D., Angellotti, G., Conigliaro, A., Carfi Pavia, F., D'Agostino, F., Contardi, M., Mauceri, R., Alessandro, R., Campisi, G., and De Caro, V. (2020). Development of a Multifunctional Bioerodible Nanocomposite Containing Metronidazole and Curcumin to Apply on L-PRF Clot to Promote Tissue Regeneration in Dentistry. Biomedicines *8*, 425. https://doi.org/10.3390/biomedicines8100425.

68. Han, X., Xue, Y., Lou, R., Ding, S., and Wang, S. (2023). Facile and efficient chitosan-based hygroscopic aerogel for air dehumidification. Int. J. Biol. Macromol. *251*, 126191. https://doi.org/10.1016/j.ijbiomac.2023.126191.

69. Wójcik-Pastuszka, D., Stawicka, K., Drys, A., and Musial, W. (2023). Influence of HA on Release Process of Anionic and Cationic API Incorporated into Hydrophilic Gel. Int. J. Mol. Sci. *24*, 5606. https://doi.org/10.3390/ijms24065606.

70. Briggs, F., Browne, D., and Asuri, P. (2022). Role of Polymer Concentration and Crosslinking Density on Release Rates of Small Molecule Drugs. Int. J. Mol. Sci. *23*, 4118. https://doi.org/10.3390/ijms23084118.

71. Kadeřábková, N., Mahmood, A.J.S., and Mavridou, D.A.I. (2024). Antibiotic susceptibility testing using minimum inhibitory concentration (MIC) assays. NPJ Antimicrob. Resist. *2*, 37. https://doi.org/10.1038/s44259-024-00051-6.

72. Liang, F., Sun, C., Li, S., Hou, T., and Li, C. (2021). Therapeutic effect and immune mechanism of chitosan-gentamicin conjugate on Pacific white shrimp (Litopenaeus vannamei) infected with Vibrio parahaemolyticus. Carbohyd Polym *269*, 118334. https://doi.org/10.1016/j.carbpol.2021.118334.

73. Miller, A.W., and Richardson, L.L. (2015). Emerging coral diseases: a temperature-driven process? Mar. Ecol. *36*, 278–291. https://doi.org/10.1111/maec.12142.

74. Alvarez-Filip, L., Estrada-Saldívar, N., Pérez-Cervantes, E., Molina-Hernández, A., and González-Barrios, F.J. (2019). A rapid spread of the stony coral tissue loss disease outbreak in the Mexican Caribbean. PeerJ *7*, e8069. https://doi.org/10.7717/peerj.8069.

75. Walker, B.K., Turner, N.R., Noren, H.K.G., Buckley, S.F., and Pitts, K.A. (2021). Optimizing Stony Coral Tissue Loss Disease (SCTLD) Intervention Treatments on Montastraea cavernosa in an Endemic Zone. Front. Mar. Sci. *8*. https://doi.org/10.3389/fmars.2021.666224.

76. Barton, J.A., Willis, B.L., and Hutson, K.S. (2017). Coral propagation: a review of techniques for ornamental trade and reef restoration. Rev. Aquac. *9*, 238–256. https://doi.org/10.1111/raq.12135.

77. Hughes, T.P., Baird, A.H., Morrison, T.H., and Torda, G. (2023). Principles for coral reef restoration in the anthropocene. One Earth *6*, 656–665. https://doi.org/10.1016/j.oneear.2023.04.008.

78. Ridlon, A.D., Grosholz, E.D., Hancock, B., Miller, M.W., Bickel, A., Froehlich, H.E., Lirman, D., Pollock, F.J., Putnam, H.M., Tlusty, M.F., et al. (2023). Culturing for conservation: the need for timely investments in reef aquaculture. Front. Mar. Sci. *10*, 1069494. https://doi.org/10.3389/fmars.2023.1069494.

79. Vega Thurber, R.L., Silva, D., Speare, L., Croquer, A., Veglia, A.J., Alvarez-Filip, L., Zaneveld, J.R., Muller, E.M., and Correa, A.M.S. (2025). Coral Disease: Direct and Indirect Agents, Mechanisms of Disease, and Innovations for Increasing Resistance and Resilience. Ann. Rev. Mar. Sci *17*, 227–255. https://doi.org/10.1146/annurev-marine-011123-102337.

80. Suggett, D.J., Edwards, M., Cotton, D., Hein, M., and Camp, E.F. (2023). An integrative framework for sustainable coral reef restoration. One Earth *6*, 666–681. https://doi.org/10.1016/j.oneear.2023.05.007.

81. Studivan, M.S., Eckert, R.J., Shilling, E., Soderberg, N., Enochs, I.C., and Voss, J.D. (2023). Stony coral tissue loss disease intervention with amoxicillin leads to a reversal of disease-modulated gene expression pathways. Mol. Ecol. *32*, 5394–5413. https://doi.org/10.1111/mec.17110.

82. Lupo, A., Coyne, S., and Berendonk, T.U. (2012). Origin and Evolution of Antibiotic Resistance: The Common Mechanisms of Emergence and Spread in Water Bodies. Front. Microbiol. *3*, 18. https://doi.org/10.3389/fmicb.2012.00018.

83. Cabello, F.C. (2006). Heavy use of prophylactic antibiotics in aquaculture: a growing problem for human and animal health and for the environment. Environ. Microbiol. *8*, 1137–1144. https://doi.org/10.1111/j.1462-2920.2006.01054.x.

84. Kalhapure, R.S., Suleman, N., Mocktar, C., Seedat, N., and Govender, T. (2015). Nanoengineered Drug Delivery Systems for Enhancing Antibiotic Therapy. J. Pharm. Sci. *104*, 872–905. https://doi.org/10.1002/jps.24298.

85. Gao, P., Nie, X., Zou, M., Shi, Y., and Cheng, G. (2011). Recent advances in materials for extended-release antibiotic delivery system. J. Antibiot. *64*, 625–634. https://doi.org/10.1038/ja.2011.58.

86. Favero M, C.K. (2020). Creation and Release Profiles of Novel Biodegradable Ointments for Lesion Based and Whole Colony Treatment Methods to be Utilized in the Response to Stony Coral Tissue Loss Disease (SCTLD). Florida DEP. https://floridadep.gov/sites/default/files/Creation%20and%20Release%20Profiles%20of%20Novel%20Biodegradable%20Ointments%20for%20Lesion%20Based%20and%20Whole%20Colony%20Treatment%20Methods%20to%20be%20Utilized%20in%20the%20Response%20to%20SCTLD_0.pdf.

87. Forrester, G.E., Arton, L., Horton, A., and Aeby, G. (2024). The relative effectiveness of chlorine and antibiotic treatments for stony coral tissue loss disease. Front. Mar. Sci. *11*. https://doi.org/10.3389/fmars.2024.1465173.

88. Ritger, P.L., and Peppas, N.A. (1987). A simple equation for description of solute release I. Fickian and non-fickian release from non-swellable devices in the form of slabs, spheres, cylinders or discs. J. Contr. Release *5*, 23–36. https://doi.org/10.1016/0168-3659(87)90034-4.

89. Ritger, P.L., and Peppas, N.A. (1987). A simple equation for description of solute release II. Fickian and anomalous release from swellable devices. J. Contr. Release *5*, 37–42. https://doi.org/10.1016/0168-3659(87)90035-6.

90. Wijmans, J.G., and Baker, R.W. (1995). The solution-diffusion model: a review. J. Membr. Sci. *107*, 1–21. https://doi.org/10.1016/0376-7388(95)00102-I.

91. Topaz, M., Athamna, A., Ashkenazi, I., Shpitz, B., and Freimann, S. (2021). In-vitro model for bacterial growth inhibition of compartmentalized infection treated by an ultra-high concentration of antibiotics. PLoS One *16*, e0252724. https://doi.org/10.1371/journal.pone.0252724.

92. Tian, Q., Zhou, W., Cai, Q., Pan, X., Ma, G., and Lian, G. (2024). Bi-layered oil encapsulates formed by polydopamine-supported in situ complex coacervation: Investigation of structure formation and sustained release performance. Colloids Surf. *692*, 133976. https://doi.org/10.1016/j.colsurfa.2024.133976.

93. Munn, C.B. (2015). The Role of Vibrios in Diseases of Corals. Microbiol. Spectr. *3*. https://doi.org/10.1128/microbiolspec.VE-0006-2014.

94. Kolle, S., Ahanotu, O., Meeks, A., Stafslien, S., Kreder, M., Vanderwal, L., Cohen, L., Waltz, G., Lim, C.S., Slocum, D., et al. (2022). On the mechanism of marine fouling-prevention performance of oil-containing silicone elastomers. Sci. Rep. *12*, 11799. https://doi.org/10.1038/s41598-022-15553-4.

95. Olio di semi di Girasole Coop. https://www.coop.it/il-prodotto-coop/coop/olio-e-aceto/alimentari-confezionati/olio-di-semi/olio-di-semi-di-girasole-1-l.

96. The European Committee on Antimicrobial Susceptibility Testing - EUCAST 2025. https://www.eucast.org/newsiandr.

97. Ambrosini, R., Corti, M., Franzetti, A., Caprioli, M., Rubolini, D., Motta, V. M., Costanzo, A., Saino, N., and Gandolfi, I. (2019). Cloacal microbiomes and ecology of individual barn swallows. FEMS Microbiol. Ecol. *95*, fiz061. https://doi.org/10.1093/femsec/fiz061.

98. Callahan, B.J., McMurdie, P.J., Rosen, M.J., Han, A.W., Johnson, A.J.A., and Holmes, S.P. (2016). DADA2: High-resolution sample inference from Illumina amplicon data. Nat. Methods *13*, 581–583. https://doi.org/10.1038/nmeth.3869.

99. Costanzo, A., Ambrosini, R., Franzetti, A., Romano, A., Cecere, J.G., Morganti, M., Rubolini, D., and Gandolfi, I. (2022). The cloacal microbiome of a cavity-nesting raptor, the lesser kestrel (Falco naumanni). PeerJ *10*, e13927.